561

Fermilab Library
0 1160 0038847 4

MIDWESTERN UNIVERSITIES RESEARCH ASSOCIATION

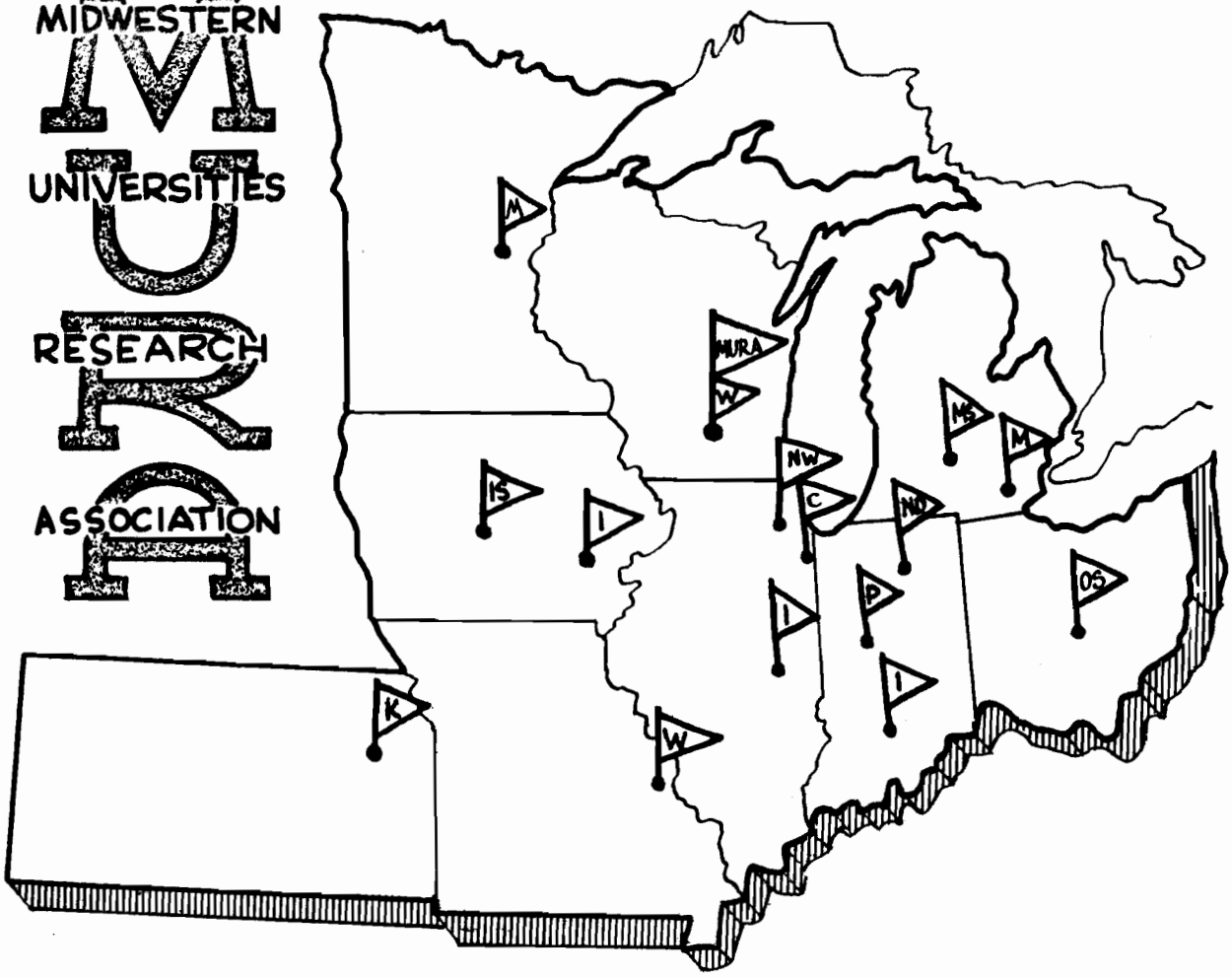

COMPUTATIONAL RESULTS PERTAINING TO USE OF A TIME-DEPENDENT MAGNETIC FIELD PERTURBATION TO IMPLEMENT INJECTION OF EXTRACTION IN A FFAG SYNCHROTRON BY USE OF THE $\nu_r = N/3$ RESONANCE

L J LASLETT AND K R SYMON

REPORT **NUMBER** 561

LEGAL NOTICE

This report was prepared as an account of Government sponsored work. Neither the United States, nor the Commission, nor any person acting on behalf of the Commission:

A. Makes any warranty or representation, express or implied, with respect to the accuracy, completeness, or usefulness of the information contained in this report, or that the use of any information, apparatus, method, or process disclosed in this report may not infringe privately owned rights; or

B. Assumes any liabilities with respect to the use of, or for damages resulting from the use of any information, apparatus, method, or process disclosed in this report.

As used in the above, "person acting on behalf of the Commission" includes any employee or contractor of the Commission to the extent that such employee or contractor prepares, handles or distributes, or provides access to any information pursuant to his employment or contract with the Commission.

Printed in USA. Price $2.00. Available from the

Office of Technical Services
U. S. Department of Commerce
Washington 25, D. C.

MURA-561
UC-28, Particle Accelerators and
High Voltage Machines
TID-4500(14th Edition)

MIDWESTERN UNIVERSITIES RESEARCH ASSOCIATION*

2203 University Avenue, Madison, Wisconsin

COMPUTATIONAL RESULTS PERTAINING TO USE OF A TIME-DEPENDENT MAGNETIC FIELD PERTURBATION TO IMPLEMENT INJECTION OR EXTRACTION IN A FFAG SYNCHROTRON BY USE OF THE ν_r = N/3 RESONANCE**

L. J. LASLETT*** AND K. R. SYMON****

March 7, 1960

ABSTRACT

The use of the ν_r = N/3 resonance to implement injection (or extraction) in a FFAG accelerator is examined and computational examples of some of the expected performance features are presented. The field of the accelerator is considered to be perturbed by a "field bump", whose period is equal to three periods of the basic (unperturbed) magnet structure, so that the radial oscillations represented by particle trajectories with amplitudes near the stability limit undergo a phase change of substantially $2\pi/3$ in passing through one sector of the unperturbed machine and a change of 2π in the basic period of the perturbed accelerator. It is shown that the boundary of the stable area in radial phase space, which normally is roughly triangular in the unperturbed accelerator, can be opened up at one of the vertices of this separatrix by a suitably-phased perturbation of the type described and that through the fixed point in this region of the diagram a new, modified separatrix will pass to enclose the stable phase area of the perturbed accelerator. Particles injected so that the initial portions of their phase trajectories pass around this latter phase area will be captured, with full phase density, as the perturbation is decreased (ultimately to zero) and as the stable phase area, in consequence, becomes enlarged.

*AEC Research and Development Report. Research supported by the U. S. Atomic Energy Commission, Contract No. AT(11-1)-384.

**A preliminary report of this work was given in the Proceedings of the International Conference on High-Energy Accelerators and Instrumentation (CERN, Geneva, 1959), pp. 38-47. MURA-546.

***Iowa State University, Ames, Iowa.

****On leave from the University of Wisconsin, Madison, Wisconsin.

It is seen that injection with full phase density may be expected if the injector at all times covers the entire region of phase space from which particles must originate in order to surround the growing phase area of the accelerator. Computational examples, with simplified equations of motion, show that the region which thus must be covered by the injector can be that enclosed by a boundary of rather simple shape, and is substantially free of filamentation, if injection occurs every three sectors (as in a three-sector accelerator). It also is found, however, that the requisite phase area to be covered by the injector becomes quite tortuous if transformed through an additional three sectors, as would be required to define the area needed with six-sector injection. The inclusion of axial motion in the computational examples showed that an orderly, efficient transfer of phase volume into the stable region of the unperturbed accelerator could be achieved by this method with three-sector injection and that the phase region which then should be covered by the injector again was enclosed by a simple boundary. Examples are given of phase curves which are similar in their essential topological features to those used in the aforementioned study but which represent the dynamics of radial motion in a spirally-ridged FFAG accelerator, the field-modification which was applied as a perturbation in this case being taken, for convenience, as an additional scaling field which follows the same logarithmically-spiralling pattern as that characterizing the unperturbed accelerator.

I. MOTIVATION

In the design of circular accelerators it is often of very great importance to inject efficiently if satisfactory performance is to be achieved, and this aspect of the design certainly warrants explicit attention in consideration of FFAG synchrotrons[1-3] intended for the production of very high current beams.[2, 4, 5] Many of the considerations which apply to the injection process also apply to certain extraction problems, since what is basically involved is an orderly transfer of phase space between regions exterior and interior to the accelerator.

In the present paper we direct our attention to a simplified problem which may be considered as the idealization of a possible method for injection into a fixed-field synchrotron, employing a secularly-changing (decreasing) perturbation of the magnetic field but without the intervention of acceleration mechanisms. It may be mentioned, however, that the specific problem considered here evidently consitutes a rather realistic description, in reverse, of an attractive method of beam extraction from a (three-sector) spiral ridge cyclotron in which the aforementioned secular change in effect is achieved by acceleration of the beam into a region of modified magnetic field.[6] With either interpretation, a fundamental feature of the present work is, as we shall see, that the essential non-linear character of the equations of motion is exploited, the dominating non-linear resonance being specifically that for which σ_r, the phase shift per sector of the radial betatron oscillations, approaches $2\pi/3$ in this case

II. GENERAL DESCRIPTION OF THE METHOD

As is well known, the inherent non-linear character of the equations for the betatron oscillations in FFAG accelerators can impose very definite limits to the amplitudes of stable oscillations. In cases such that the phase change of the radial betatron oscillations in one sector (σ_r) is near $2\pi/3$, the limitation is primarily controlled by a quadratic term in the equations of motion and the stability limits then typically are indicated by the excursions of unstable equilibrium orbits having a period equal to three sectors. The features of the radial betatron motion are conveniently represented by phase plots,[1,2,7] employing as axes the quantities $x \equiv (r - r_0)/r_0$ and $p \equiv dx/d\theta$ with r_0 denoting a reference radius, on which the motion of a particular particle is depicted once per period of the magnet structure to form closed "invariant phase curves" in the stable region. The unstable equilibrium orbits are then represented by fixed points, through which passes the separatrix which bounds the roughly triangular region of stability (cf. Fig. 1, in which conveniently scaled coordinates are used).*

In the case which will be of interest here we shall impose a field perturbation, whose wavelength is equal to three periods of the magnet structure, suitably phased so as to "open up" the phase plot in the region of one of the unstable fixed points. The invariant curves which pass through the other two fixed

*In this discussion we have tacitly assumed the existence of the so called "invariant phase curves", although actually over long intervals of time the motion may be found to show a considerable departure from such regular motion and, similarly, the boundary between "stable" and "unstable" regions becomes imprecisely defined.[8]

points then no longer intersect at the first fixed point and a separate separatrix serves to define such stable area as may still remain when the perturbation is not too large (Fig. 2.). A region of phase space is thus created within which the phase points move through substantially the entire region just outside the region of stability -- if the stable region is now caused to grow, as a result of decreasing the magnitude of the perturbation, phase points may be expected to be transferred to the interior of the stable region with the same density as initially is present outside.

It is attractive, then, to consider the application of a perturbation which initially is more than sufficiently large to cause the stable region to disappear completely and which is steadily decreased to create a region of stability which ultimately becomes that of the unperturbed accelerator. By an appropriately located injector, particles may now be caused to "flood" the boundary region which surrounds the stable area as it is created and one may expect thereby to fill this area with a phase density equal to that available from the injector. For efficient injection it would be desirable, of course, to inject only into that region of space from which particles will be captured. It would be convenient, moreover, if this region which must be covered by the injector were to behave in a sufficiently orderly way as to obviate the need to change the direction of the injected beam in accordance with an elaborate programme synchronized with the changing strength of the magnetic-field perturbation. In some cases, however, the area of phase space which the injector can cover may be sufficiently great as not to be a fundamental limitation, although the phase density which it can provide should be used efficiently, and in such cases a programmed scan would

either be unnecessary or, at worst, not critical.

To examine the performance which could be achieved by this method in any particular case, a natural initial step is the determination of the phase plots associated with static perturbations representative of the time-dependent perturbation which it is intended to apply. Useful orientation in simple cases can be obtained at this point by analytic means, although computer studies of course can be helpful. One may then proceed with computations in which the time-dependent perturbation is present, to determine the regions of phase-space from which patricles will be captured at various stages of the process. If these regions can be caused to fall at locations accessible to an injector system, and if they neither shift about violently nor show more than trivial filamentation, the proposed method in principle could be said then to be practicable. Similarly, such an orderly transferral of phase space could be considered as indicating the potential utility of the inverse process[6] for beam extraction.

In the following sections we describe the results obtained in some initial studies of this injection method, the work so far having been confined to analysis and computations* for equations chosen for convenience to be of a rather simple

*The computations were performed with the MURA I. B. M. -704 computer, using programs prepared by Dr. J. N. Snyder, now at the University of Illinois, and Mr. M. Storm, the present Head of the MURA Computer Section. We are indebted to Dr. Snyder, Mr. Storm, and others associated with the Computer Section for their invaluable help and continual cooperation during all phases of the computer work.

form, but which it is believed should depict the essential features of more exact equations representative of particle motion in a spirally-ridged FFAG accelerator. Also, for reasons of simplicity, the field perturbation is taken to fall linearly to zero and to remain zero thereafter.

III. THE DIFFERENTIAL EQUATIONS EMPLOYED

In the theory of spirally-ridged FFAG accelerators the radial betatron motion, about the stable equilibrium orbit, may be conveniently represented by[9]

$$\frac{d^2u}{d\theta^2} + \left[a + b\cos N\theta\right] u = \frac{1}{2} b_1(\theta)\, u^2 + \ldots, \tag{1}$$

where u denotes the departure from the stable equilibrium orbit, in units of the radius,

$$a \cong (k+1) - \frac{1}{2}\left(\frac{f}{wN}\right)^2, \tag{2a}$$

$$b \cong f/w, \text{ and} \tag{2b}$$

$$b_1(\theta) \cong -(f/w^2)\sin N\theta, \tag{2c}$$

in terms of the parameters f, w, and N characterizing the accelerator.[2, 9]

By introducing the scaled variables

$$s = (N/2)\theta + \pi/4 \tag{3a}$$

$$v = u/w, \tag{3b}$$

Eqn. (1) assumes form

$$\frac{d^2v}{ds^2} + 4\left[\frac{a}{N^2} + \frac{f}{wN^2}\sin 2s\right] v - \frac{1}{2}\left(\frac{4f}{wN^2}\right)(\cos 2s)\, v^2 = 0. \tag{4}$$

Although it is possible by a suitable transformation[10, 11] to remove the alternating gradient feature of the linear term, we do not believe it necessary to make this transformation explicitly in the present work but may consider the essential features of interest here to be represented by use of the smooth approximation equivalent of this coefficient.[1, 11] In what follows, therefore, we shall take the unperturbed radial motion as represented adequately by

$$\frac{d^2 v}{ds^2} + \left(\frac{2\nu_r}{N}\right)^2 v - \frac{B}{2}(\cos 2s)\, v^2 = 0. \tag{5}$$

The type of perturbation which will be effective in implementing injection by the method previously described will be, in essence, a periodic variation of the field strength along the equilibrium orbit, with a period equal to the length of three magnet sectors. We thus include the perturbation in the differential equation by writing

$$\frac{d^2 v}{ds^2} + \left(\frac{2\nu_r}{N}\right)^2 v - \frac{B}{2}(\cos 2s)\, v^2 - \lambda \cos\frac{2s}{3} = 0, \tag{6}$$

where λ serves to measure the strength of the perturbation. Illustrations of coupled motion may be obtained by considering the pair[9, 12]

$$\frac{d^2 v}{ds^2} + \left(\frac{2\nu_r}{N}\right)^2 v - \frac{B}{2}(\cos 2s)\,(v^2 - y^2) - \lambda \cos\frac{2s}{3} = 0 \tag{7a}$$

$$\frac{d^2 y}{ds^2} + \left(\frac{2\nu_z}{N}\right)^2 y + B(\cos 2s)\, vy = 0, \tag{7b}$$

which are derivable from a Hamiltonian

$$\mathcal{H} = \frac{p_v^2}{2} + \frac{p_y^2}{2} + 2\left(\frac{\nu_r}{N}\right)^2 v^2 + 2\left(\frac{\nu_z}{N}\right)^2 y^2$$
$$- \frac{B}{6}(\cos 2s)\, v^3 + \frac{B}{2}(\cos 2s)\, vy^2 - \lambda v \cos\frac{2s}{3}, \tag{8}$$

with y denoting the axial coordinate, in the same units as v and with

$$p_v \equiv dv/ds \tag{9a}$$

$$p_y \equiv dy/ds\,. \tag{9b}$$

It will be observed that as $\nu_r/N \rightarrow 1/3$ the stable solutions to Eqn. (5) will become increasingly limited by the $2\pi/3$ resonance, in which the betatron oscillations experience a phase change of $2\pi/3$ in progressing through one magnet sector. Similarly, in progressing through one period of the perturbed structure (i.e., through 3 sectors) the corresponding phase change would approach 2π and the stability limitation for the solution to Eqn. (6) could be regarded in this sense as due to an integral resonance. In examining particular examples of solutions to Eqns. (7a, b) we shall, in what follows, specifically employ

$$\nu_r/N = 0.3 \tag{10a}$$

$$\nu_z/N = 0.0992 \tag{10b}$$

$$B = 1.15 \tag{10c}$$

and λ will assume values in the range $0 \leq \lambda < 0.025$. (10d)

IV. THE SOLUTIONS TO THE RADIAL EQUATION FOR A STATIC PERTURBATION

The solution to Eqn. (5) —i.e., of solutions to Eqn. (6) with $\lambda = 0$ — can be estimated by use of the analytic methods described by J. Moser[13] and the unstable equilibrium orbits alternatively can be obtained rather accurately by substitution of a trial solution and use of harmonic balance (Table I).[14]

TABLE I

Location of Unstable Fixed Points for Eqn. (5) at s = 0, as obtained (i) by Application[14] of the Moser Method,[13] through terms of order $(\nu/N-1/3)^2$; (ii) by Harmonic Balance[14] with Terms of Argument 2s/3, 2s, and 10s/3; and (iii) Computationally.

Point	Calc.[14] by Moser Method		Cal.[14] with Trial Function		Computational Results	
	v	p_v	v	p_v	v	p_v
1	-0.5132	0	-0.5237	0	-0.5238	0
2, 3	0.2256	$\pm$0.2667	0.2319	$\pm$0.2783	0.2320	$\pm$0.2789

The direct application of the Moser procedure in the case $\lambda \neq 0$ is more tedious, since the initial transformation required to eliminate the forcing term $-\lambda \cos \frac{2s}{3}$ introduces time-dependent (A-G) terms into the coefficient of v, but a similar, somewhat simplified, analytic method can be applied conveniently and, moreover, the fixed points again can be estimated quite well by use of harmonic balance (Table II).[15]

TABLE II

Location of Stable and Unstable Fixed Points for Eqn. (6) at $s = 0$, with $\lambda = 0.006$

Point	Analytic Calc.[15]		Calc. with Trial Function.[15]		Computational Results	
	v	p_v	v	p_v	v	p_v
Stable	-0.08362	0	-0.083803	0	-0.083802	0
1	-0.44855	0	-0.44336	0	-0.44345	0
2, 3	0.2161	± 0.2841	0.22451	± 0.3023	0.22457	± 0.3030

The detailed characteristics of phase plots which are obtained for any particular value of λ depend, of course, on the particular value of s (mod. 3π) -- or of θ (mod. $6\pi/N$)--to which they apply, but the topological features are independent of s (compare Figs. 2 and 3, which respectively apply to $s = 0$ and to $s = \pi/2$, mod. 3π). It is found, firstly, that the application of the perturbation ($\lambda > 0$) does open up, as desired, the phase curves which originally intersected at one of the unstable fixed points and, secondly, that this fixed point and the stable fixed point approach one another as the strength of the perturbation is increased (Fig. 4), to result in the complete disappearance of the stable region at a critical strength of the perturbation, $\lambda_c = 0.01136$ (Fig. 5).*

It may be noted in passing that, for small λ, the locations of these two fixed

*Additional phase plots are shown in reference 16. Figures 6-11 further illustrate the evolution of phase plots of the form of Fig. 2 as the reference point is taken as $s = 0, \pi/2, \ldots 5\pi/2$

points which lie on the $p_v = 0$ axis when $s = 0$ (mod. 3π) may be estimated by[15]

$$v_1(\lambda) \cong -\frac{\lambda}{4/9 - (2\nu_r/N)^2} \tag{11a}$$

$$v_2(\lambda) \cong v_{2,0} + \frac{\lambda}{4/9 - (2\nu_r/N)^2}, \tag{11b}$$

where $v_{2,0}$ denotes the coordinate value of the unstable fixed point when $\lambda = 0$. A parabolic fit, tangent to the lines (11a, b) at $\lambda = 0$, may be written

$$\lambda = \frac{v \cdot \left[v - v_{2,0}\right]}{v_{2,0}} \cdot \left[4/9 - (2\nu_r/N)^2\right], \tag{12}$$

for which the maximum value of λ,

$$\lambda_c = \left[1/9 - (\nu_r/N)^2\right]\left[-v_{2,0}\right], \tag{13a}$$

is attained at

$$v_c = \frac{1}{2} v_{2,0}. \tag{13b}$$

With $\nu_r/N = 0.3$ and $-v_{2,0} = 0.5238$, Eqns. (13a, b) suggest

$$\lambda_c = 0.01106 \tag{14a}$$

$$v_c = -0.2619, \tag{14b}$$

which may be compared with the computational results

$$\lambda_c = 0.01136 \tag{14a'}$$

$$v_c = -0.2650. \tag{14b'}$$

We note, finally, that suitably injected particles --e.g., with their initial phase points lying in the region A of Fig. 2 --will move such that their phase points pass completely around the stable region which is formed as the perturbation is being removed. We may expect, therefore, that particles captured in this way will fill the stable region with a phase density equal to the maximum theoretically attainable.

V. INJECTION WITH A SECULARLY-DECREASING PERTURBATION

We imagine the injector situated physically at radii less than those of the stable region into which it is desired to inject--say with $v \leq -0.55$ at $s = 0$ (Fig. 1)--to avoid any interference by the injector with the captured beam. With an assumed particular value for the rate of decrease of the perturbation, one then seeks to find, by digital computations, the regions of phase space within which particles may be started, at various initial values of λ, to become captured within the final stable region. The possible difficulties which conceivably could be discovered in such a search would be:

(i) an appreciable fraction of the region of interest might be found not to pass through regions to the left of $v = -0.55$;

(ii) the location of the region with respect to momentum, p_v, might vary strongly with the initial value of λ;

(iii) the region in phase space might be found to be seriously filamented; and

(iv) the coupling between radial and axial motion may be found to play a more dominant rôle than is usually the case with stable motion, with a consequent complexity of the four-dimensional phase space and of its projections onto the radial and axial sub-spaces.

A. Characteristics when only radial oscillations are present.

For an initial computational investigation it is convenient to confine one's attention to motion in the median plane (axial oscillations absent). One may then commence by finding the range of momenta, p_v, which, at $v = -0.55$ and for various representative initial values of λ, lead to capture into the stability region. From such values other suitable initial conditions could be found by

integration backwards in s, to obtain a transformed set of points situated at smaller radii, although with a three-sector accelerator (or with injectors located at every third sector around a larger accelerator) such a reverse transformation should only be carried through a three-sector interval in order to avoid the inclusion of points which would encounter physical interference by the injector structure. The region between these two lines in the radial phase-plane--i.e., between the lines at $v = -0.55$ and its transform through $\Delta s = -3\pi$--can then be explored to find the boundaries of the regions suitable for injection.

Such a computational survey of the radial phase-plane has been made for the case $d\lambda/ds = -0.002/3\pi = -2.122 \times 10^{-4}$, which corresponds to a linear decrease of the perturbation at a rate such that the strength of the perturbation would decrease from its critical value, λ_c, to zero in the time taken by the particle to traverse 17 sectors of the unperturbed machine. The results of this survey are summarized below.

For the initial value $v = -0.55$, the range of "momenta", p_v, within which particles are captured for various initial values of λ, are as shown in Fig. 12. It is noted that the useful values of λ extend considerably beyond the critical value, λ_c, since λ will decrease during the time the phase points of the particles progress through the region wherein the stable area is being established. As mentioned above, each such range of values was then projected backward in s to give a second locus of values, applicable three sectors earlier (and for a value of λ greater by 0.002). The intermediate region of the phase-plane, between $v = -0.55$ and its transform, was then surveyed to obtain results of which those portrayed in Fig. 13 are typical. For the particular case

studied, filamentation of the "phase fluid" was almost entirely absent throughout the entire phase area which was mapped out in this way, although in a few cases the computations showed evidence of an apparent incipient filamentation developing along the lower edge of the region (Fig. 14, insert).*

The areas of radial phase space which thus should be covered by the injector were obtained from curves of the type shown in Fig. 13. These areas, $A(\lambda)$, have been plotted, vs. the initial value of λ, in Fig. 15 and to lead to the integrated result

$$\int A(\lambda)\, d\lambda = 0.00046. \tag{15}$$

If the injector is capable of delivering n particles per unit area of radial phase space per unit time, the total number of particles which thus could be successfully injected by this means would be

---

*A more detailed examination of the progress of points (such as those designated by "c" and "d" in Fig. 14) which suggested the occurance of filamentation led to the following interpretation of the observed behavior. Initial conditions lying just below the main shaded area of Fig. 14 lead to trajectories which pass around the growing stable region of the v, p_v plane before this area has grown sufficiently to capture such particles. The trajectories of particles with initial conditions such as those represented by the points "c" and "d" of Fig. 14, however, pass sufficiently close to the fixed points situated in the right-hand portion of the phase diagran -- e.g., close to, but inside of, point B(or C) of Fig. 6 -- that the progress of such phase points becomes quite slow and the stable area grows to capture these particles before they reach a region from which they could escape (see Fig. 35).

$$\eta = \int n\ A(\lambda)\ dt$$

$$= \frac{n}{|d\lambda/dt|} \int A(\lambda)\ d\lambda$$

$$= \frac{n}{\omega N} \frac{2}{|d\lambda/ds|} \int A(\lambda)\ d\lambda$$

$$= \frac{n}{\omega N} \frac{6\pi}{0.002}\ 0.00046$$

$$= 4.3 \frac{n}{\omega N}, \tag{16}$$

where $\omega \equiv d\theta/dt$ denotes the angular velocity of the particles in the accelerator. This result may be compared with the maximum theoretically obtainable by direct injection, during a three-sector interval, into the stable area without violation of Liouville's theorem, namely

$$\eta = \frac{n}{\omega}\left(\frac{6\pi}{N}\right) \cdot \left[\text{Area of stable phase plot}\right]$$

$$= \frac{n}{\omega}\left(\frac{6\pi}{N}\right)(0.223)$$

$$= 4.2 \frac{n}{\omega N}. \tag{17}$$

Since the estimates expressed by Eqns. (16) and (17) are effectively identical, it is evident that excellent efficiency of injection into radial phase space has been obtained from the region mapped in this example, although with injection through more than three sectors or with more complicated differential equations a more pronounced filamentation or dispersal of phase space might well

develop to present practical difficulties.* The transfer of radial phase space from outside the stable region to the interior appears to be quite orderly in the case which we examined and so encourages a continuation of the investigation of this injection (or extraction) method.

---

* An attempt was made in the present example to extend the area leading to capture back through an additional three sectors--i.e., through an additional $\Delta s = -3\pi$--in the interest of examining the possibility of injection at intervals greater than three sectors without loss of phase density. It was found, as might have been anticipated, that the additional useful area of phase space (from which particles would be successfully captured) became very slender or "stringy". In addition, moreover, this slender acceptance area followed a rather tortuous locus. In particular, the region for which $\lambda_o = 0.0174375$ at $s = 3\pi/32$ was followed backwards in s through an interval -3π to determine the initial conditions which, with $\lambda_o = 0.0194375$, would feed the area in question. This area, which accordingly was subjected to the reverse transformation (through $\Delta s = -3\pi$) for the purpose of this examination, thus was specifically that of Fig. 27, to which reference is made in the following paragraph of the text. The additional area which the reverse transformation mapped out in this way, for $\lambda = 0.0194375$, was found to extend virtually to $v = -8$ and to positive values of about $4\frac{2}{3}$, while going to momentum values (p_v) of -3.45 and about -4.2, respectively. The difficulties which this extension of the phase area would imply for the possible application of the method to such six-sector injection almost undoubtedly would become exacerbated by the inclusion of axial motion in the dynamics.

The exact azimuth at which the injector should be situated might be adjusted, in practice, to achieve a convenient match to the properties of the injector; it probably would be convenient to select a location where the useable values of p_v vary the least during the interval that the secularly-changing perturbation is being employed and for which the phase diagrams defining initial conditions which lead to capture might be similar to that shown in Fig. 16 [for which $s = 3\pi/32$, $\lambda(s=3\pi/32) = \lambda(s=0) - \frac{0.002}{3\pi}\Delta s = 0.0165 - 0.0000625 = 0.0164375$, and $d\lambda/ds = -\frac{0.002}{3\pi}$.] (Phase plots corresponding to this angle, $s = 3\pi/32$, are shown for constant values of λ, $\lambda = 0$ and $\lambda = 0.006$, in Figs. 17 and 18; similarly, Figs. 19 and 20 apply to $s = \pi/2$ and the constant values $\lambda = 0$ or $\lambda = 0.006$, respectively.) A series of graphs defining initial conditions at $s = 3\pi/32$ which lead to capture are shown in Figs. 21-30, for cases in which λ decreases to zero from initial values (at $3\pi/32$) of 0.0054375, 0.0074375, ... 0.0234375. These curves, and that of Fig. 16 presented earlier, all show the acceptable momenta to lie near $p_v = 0$. If the location $s = 3\pi/32$ were then actually selected for operation, the areas of interest would be similar to those of Figs. 21-30, slightly modified so that the right-hand boundary is located at a fixed value of v (as, for example, v = -0.55) -- typical of such a modified graph is Fig. 31, which may be compared with Fig. 27.

B. The effect of axial motion.

As in other accelerator investigations, the inclusion of the additional, axial, degree-of-freedom in the present study introduces considerable complication and requires a rather extended amount of computation if a comprehensive

picture is to be obtained. The importance of including the axial motion in such studies is clear, however, as has been emphasized by Terwilliger in connection with a computational investigation[17, 18] of a method which proved to afford a promising means of beam extraction from a spiral sector accelerator.[19] As we shall see, the results which have been obtained for the present problem do indicate that, as expected, the axial motion exerts a marked effect on the performance and this influence must be kept in mind when evaluating the utility of the method if efficient injection into the entire stability region of the accelerator is required.

A search for the y-stability limit for solutions to Eqns. (7a, b) in the absence of the perturbation indicated that this limit lay between 0.72 and 0.85 if the amplitude of the radial motion was initially zero (i.e., corresponding to the origin of the radial phase plot shown in Fig. 1). For larger amplitudes the permissible initial axial amplitudes were somewhat reduced, as shown in Table III.

TABLE III

Computational Estimates of Limiting Axial Amplitudes, with various initial Radial Amplitudes, for Solutions to Eqns. (7a, b)

with $\lambda = 0$.

$$\left[p_{v_o} = p_{y_o} = 0\right]$$

v_o	y_o	
	Stable	Unstable
0	0.72	0.85
-0.001	0.61	0.72
-0.0025	0.52	0.61

To illustrate the influence of axial motion on the proposed injection method, we have made preliminary computations for the case in which the initial strength of the perturbation is $\lambda_o = 0.0165$ (and $d\lambda/ds = -0.002/3\pi$) and for which Fig. 13 applies in the absence of axial motion. The y-stability limits for Eqns. (7a, b) were then sought for $v_o = -0.55$ and for $v_o = -0.85$, in each case assigning to the initial radial momentum, p_{v_o}, a value near the center of the previously permissible range of values. The results of this search, summarized in Table IV, indicate that the axial stability limits for these representative cases were materially smaller than those shown in Table III.

TABLE IV

Computational Estimates of Limiting Axial Amplitudes, with representative Initial Conditions for the Radial Motion, for Solutions to Eqns. (7a, b) with $\lambda_o = 0.0165$ and $d\lambda/ds = -0.002/3\pi$.

$[p_{y_o} = 0]$

v_o	p_{v_o}	y_o	
		Stable	Unstable
-0.55	-0.13625	0.31	0.37
-0.85	-0.22	0.19	0.21

Guided by the results shown in Table IV, the range of permissible values of p_{v_o}, leading to stable motion, was then examined at $v_o = -0.55$ and at $v_o = -0.85$ for several initial axial amplitudes. The results of this survey are summarized in Table V.

TABLE V

Computational Estimates of Range of Permissible Radial Momenta, with representative initial radial and axial coordinates, for Solutions to Eqns. (7a, b) with $\lambda_o = 0.0165$ and $d\lambda/ds = -0.002/3\pi$.

$$\left[p_{y_o} = 0\right]$$

y_o	v_o	p_{v_o}			
		Unstable	Stable	Stable	Unstable
0	-0.55	-0.0775	-0.0800	-0.1925	-0.1950
0.19		-0.09	-0.10	-0.19	-0.20
0.22		-0.09	-0.10	-0.19	-0.20
0.26		-0.10	-0.11	-0.19	-0.20
0.31		-0.12	-0.13	-0.19	-0.20
0.37		-0.14	-0.15	-0.20	-0.21
0.44		-0.18	-0.19	-0.21	-0.22
0.52		-0.22	-0.23	-0.24	-0.25
0	-0.85	-0.190	-0.195	-0.245	-0.250
0.19		-0.21	-0.22	-0.25	-0.26
0.22		-0.22	-0.23	-0.26	-0.27
0.26		-0.23	-0.24	-0.27	-0.28
0.31		-0.25	-0.26	-0.28	-0.29

It is clear that axial amplitudes much smaller than those which appear in Table III result in a material reduction of the useful range of p_{v_0}. The larger values of y_0 listed in Table V are seen, moreover, to be associated with values of p_{y_0} differing from those suitable for $y_0 = 0$ and injection with values of y_0 as large as those listed near the end of each section of Table V may be of rather limited utility.

The results of the preliminary investigation described above thus indicate that it would be of interest to obtain a more definitive picture of the region of phase space which must be covered for two degrees-of-freedom if efficient, virtually complete, filling of the final stable phase volume is to be achieved. With this objective, therefore, a large number of phase points (v, p_v, y, p_y) which were considered representative of various portions of the stable region in the phase volume of the unperturbed accelerator were followed "backward" in time as the perturbation now was permitted to increase, from zero, during the course of the computation. Upon examining the computational results at intervals of 3π for the independent variable s, the appropriate phase-coordinates for injection in each case were then taken to be the values found the first time the results showed $v \leq -0.55$.

Specifically, from exploratory computations similar to those summarized in Table III, it was estimated that the stable phase volume for the unperturbed equations ($\lambda = 0$) roughly amounted to 0.060, or possibly 0.068, $\Delta v \cdot \Delta p_v \cdot \Delta y \cdot \Delta p_y$ - units. This estimated stable volume was imagined to be divided into some 512 "cells", individually of volume 0.000133, within each of which a

single (stable) point was selected as representative. By following the phase trajectories of such points, in the reverse manner described in the preceeding paragraph, then, a reasonable mapping was obtained of the region of phase space which appropriately should be covered by the injector.*

From the results of this computational survey it appeared that some 92% of the desired phase volume would be filled if three-sector injection, at $s = 3\pi/32$, covered the range**

$$-1.50 \leq v \leq -0.55 \qquad -0.492 \leq y \leq +0.492$$
$$-0.301 \leq p_v \leq +0.05 \qquad -0.65 \leq p_y \leq +0.65 \quad ;$$

similarly, and perhaps more significantly, about 88% filling would be achieved by an injector which only covered the region

$$-1.26 \leq v \leq -0.55 \qquad -0.492 \leq y \leq +0.492$$
$$-0.21 \leq p_v \leq +0.05 \qquad -0.55 \leq p_y \leq +0.55 \; .$$

Since, moreover, there evidently was considerable correlation between the required values of y and p_y, the last-mentioned final density of 88% would indeed be obtained under these circumstances if the axial phase area were covered by

---

*In the actual computations it was of course sufficient only to follow half of the points which were taken as representative of the phase-volume-elements selected, due to the invariance of the differential equations to a simultaneous change of sign of y and p_y [cf. Eqns. (7a, b)].

*The required values for λ which would prevail at injection for the successful runs of this series were embraced by the interval $0.0074375 \leq \lambda \leq 0.0214375$.

s

an injector which was somewhat "wall-eyed" axially (at $s = 3\pi/32$) in the sense of only providing full phase density within the area sketched on Fig. 32.

VI. COMPUTATIONAL EXAMINATION OF THE EQUATIONS FOR A SPIRAL-RIDGE ACCELERATOR

Since the computational work described in the previous sections employed idealized equations [namely (7a, b)], it is of interest to make a brief comparative examination of the corresponding phase plots which represent exact solutions of the dynamical equations for a spirally ridged FFAG accelerator. With this motivation attention was directed to a structure with

$$N = 33, \qquad k = 79, \qquad 1/w = 1252,$$

and with a "flutter factor" of 0.25 in the unperturbed field. For the perturbed structure it was thought to be convenient to employ a field-bump which followed the same spiral pattern as the unperturbed field except for the three-fold longer period which, as before, would be appropriate for exciting the $\nu_r = N/3$ resonance. The scaling median-plane field was thus taken to be given by an expression of the form*

---

* To permit use of existing MURA programs for the IBM-704 computer, the expression for the median-plane field was imagined as re-written in the form

$$-B_{z,o}/r^k = 1 - \frac{\lambda}{\sqrt{2}}\left\{\cos\left[\frac{1}{w'}\ln(1+x) - N'\theta\right] + \sin\left[\frac{1}{w'}\ln(1+x) - N'\theta\right]\right\} + 0.25\cos 3\left[\frac{1}{w'}\ln(1+x) - N'\theta\right],$$

where $N' = N/3 = 11$ and $1/w' = (1/w)/3 = 417.33333$.

$$-B_{z,o}/r^k = 1 + 0.25 \cos\left[\frac{1}{w}\ln(1+x) - N\Theta\right] - \lambda \cos\left\{\frac{1}{2}\left[\frac{1}{w}\ln(1+x) - N\Theta\right] - \frac{\pi}{4}\right\}, \quad (18)$$

in which a typical value of λ, sufficiently large to cause an appreciable modification of the radial phase plots, would be $\lambda \cong 0.0015$ and for which it proved of interest to plot the results at $33\Theta = 0$, mod. 6π.

The stable fixed point for the unperturbed structure [with $\lambda = 0$ in Eqn. (18)] was found to (for $33\Theta = 0$, mod. 2π) at

$$x_{FP} = -4.15 \times 10^{-5}$$
$$p_{x,FP} = -8.52_7 \times 10^{-3}$$

and the frequency of small-amplitude radial betatron oscillations was such that

$$\sigma_x \cong 0.59_7\pi \qquad (\text{or } \nu_r/N \cong 0.29_8).$$

This radial oscillation frequency is thus substantially the same as that used with the simpler Eqns. (7a, b); for the axial motion, likewise, the value of σ_y is

$$\sigma_y \cong 0.19_3\pi \qquad (\text{or } \nu_z/N \cong 0.09_7),$$

as in the previous work with Eqns. (7a, b).

The radial phase plots for the unperturbed structure approached the familiar triangular shape (Fig. 33) as the amplitude was increased, but it did <u>not</u> appear (in a reasonably careful investigation) that the rotation number then locked in to $2\pi/3$ to produce fixed points of order 3 in regions such as that designated by C on Fig. 33. It may, none-the-less, be reasonable to consider the region of x, p_x phase space which may be put to effective use to be substantially that contained within the largest solid-line phase plot on Fig. 33.

The complications which made it difficult to construct a complete orderly set of phase plots for the unperturbed structure also appear to have their effects on the results of dynamical studies when the strength of the perturbation is characterized by the illustrative value $\lambda = 0.0015$. The most important

characteristics relevant to the present investigation seem to make their appearance, however (Fig. 34). Thus, for $\lambda = 0.0015$ (and again referring the results to $33\Theta = 0$, mod. 6π), the stable fixed point is found to lie at

$$x_{FP} = -1.413 \times 10^{-4}$$

$$p_{x,FP} = -8.018 \times 10^{-3} .$$

In addition, an unstable fixed point analogous to point P of Fig. 18 appears to occur at

$$x_{FP} = -1.013_{271} \times 10^{-3}$$

$$p_{x,FP} = -8.384_{56} \times 10^{-4} .$$

Thus one might propose injecting into regions such as that outlined by the solid curve in Fig. 34, which would grow in area as the strength of the perturbation is decreased, to achieve an effective filling of the useful stable phase region which is depicted in Fig. 33 for the final unperturbed accelerator.

VII. CONCLUSIONS.

The particular injection method discussed in this paper was found to permit effecient transfer of radial phase space between regions exterior and interior to the accelerator, although complications might be expected to arise if the physical limitation imposed at the time the beam returns to the injector azimuth were deferred for longer than the three sectors considered here. The results of the method appear to show a close resemblance to those which previously[6] have indicated the potential utility of a similar perturbation for the efficient extraction of a beam from a three-sector fixed-field accelerator.

The preliminary studies of the influence of substantial axial oscillation amplitudes on the particle behavior indicated that this influence was pronounced and so might detract materially from the practicality of the method unless additional considerations, such as the limitation of axial amplitudes by the vacuum chamber or the damping of oscillation amplitudes prior to use of the method for ejection, served to limit the axial amplitudes to values considerably less that are dynamically stable in the absence of the perturbation.

It is hoped that the method and results reported here will prove suggestive of other possible methods of utilizing a secularly-changing perturbation in conjunction with the non-linear dynamical properties of the orbits, including methods in which the perturbation may have a greater period than that employed here and so would interact with a machine resonance rather than with an inherent sector resonance.

VIII. ACKNOWLEDGEMENTS.

It is a pleasure to acknowledge the assistance of Mr. Seymour J. Wolfson, a MURA summer visitor from Wayne State University, in some of the algebraic and numerical calculations connected with the analytic phases of this investigation, and to thank Mr. Igor Sviatoslavsky for assistance with some of the graphical work. We also appreciate the continued cooperation of the members of the Computer Division in implementing the computational work,[20] and are grateful to Dr. Fred E. Mills for very helpful discussions concerning basic questions relating to injection.

LIST OF REFERENCES

1. Symon, K. R., et al. Fixed-Field Alternating-Gradient Particle Accelerators. Phys. Rev., 103, p. 1837-1859, 1956.
2. Laslett, L. Jackson. Fixed-Field Alternating-Gradient Accelerators. Science, 124, p. 781-787, 1956.
3. Kerst, D. W., et al, Fixed-Field Alternating-Gradiant Particle Accelerators. Proceedings of the CERN Symposium on High Energy Accelerators and Pion Physics, 1, p. 32-35, 1956.
4. Kerst, D. W., et al. Attainment of Very High Energy by Means of Intersecting Beams of Particles. Phys. Rev., 102, p. 590-591, 1956.
5. Kerst, D. W. Properties of an Intersecting-Beam Accelerating System. Proceedings of the CERN Symposium on High Energy Accelerators and Pion Physics, 1, p. 36-39, 1956.
6. Blosser, H. G., et al. A Proposal for a Nuclear Research Facility in the Medium Energy Range Utilizing a 64" Variable Energy Multi-Particle Cyclotron. Michigan State University Department of Physics and Astronomy report, East Lansing Michigan, p. 1-135, 1958. Sect. III-A-1-c, p. 67-76.
7. Laslett, L. J. and Symon, K. R. Particle Orbits in Fixed-Field Alternating Gradient Accelerators. Proceedings of the CERN Symposium on High Energy Accelerators and Pion Physics, 1, p. 279-289, 1956.
8. Moser, Jürgen. Non-Existence of Integrals for Canonical Systems of Differential Equations. Commun. Pure & Appl. Math., 8, p. 409-436, 1955.

9. Cole, F. T. Mark V FFAG Expanded Equations of Motion. Midwestern Universities Research Association report MURA-95, Madison, 1956.

10. Courant, E. D. and Snyder, H. S. Theory of the Alternating-Gradient Synchrotron. Ann. of Phys., 3, p. 1-48, 1958. Eqns. (4.4)-(4.5), p. 18.

11. Cf. Hagedorn, R., Hine, M. G. N., and Schoch, A. Non-Linear Orbit Problems in Synchrotrons. Proceedings of the CERN Symposium on High Energy Accelerators and Pion Physics, 1, p. 237-253, 1956. Sect. III-B-1, p. 246-247.

12. Cf. Hagedorn, R. Note on an Instability on a Difference Resonance Line. Proceedings of the CERN Symposium on High Energy Accelerators and Pion Physics, 1, p. 293-294, 1956.

13. Moser, Jürgen. Stabilitätsverhalten kanonischer Differentialgleichungssysteme, Nachr. Akad. Wiss. Göttingen (Math.-Phys. Kl.), IIa, Nr. 6, p. 87-120, 1955.

14. Laslett, L. Jackson. Concerning the $\nu/N \rightarrow 1/3$ Resonance, I: Application of a Variational Procedure and of the Moser Method to the Equation $d^2v/dt^2 + (2\nu/N)^2 v + (1/2)(\sin 2t) v^2 = 0$. Midwestern Universities Research Association report MURA-452, Madison, 1959.

15. Laslett, L. Jackson and Wolfson, Seymour, J. Concerning the $\nu/N \rightarrow 1/3$ Resonance, V: Analysis of the Equation $d^2v/ds^2 + (2\nu/N)^2 v - (b/2)(\cos 2s) v^2 - \lambda \cos(2s/3) = 0$. Midwestern Universities Research Association report MURA-497, Madison, 1959.

16. Laslett, L. Jackson. Concerning the $\nu/N \rightarrow 1/3$ Re[illegible], VI: Phase Plots and Fixed Points Obtained Computationally for Several Equations Affected by the $\nu/N \rightarrow 1/3$ Resonance. Midwestern Universities Research Association report MURA-515, Madison, 1959.

17. Terwilliger, Kent M. Beam Extraction from an FFAG Synchrotron. Midwestern Universities Research A[illegible]ciation report MURA-427, Madison, 1958.

18. Jones, L. W. and Terwilliger, K. M. Beam Extraction from FFAG Accel[illegible]rators. Proceedings of the International Conference on High-Energy Accelerators and Instrumentation (CERN, Geneva, 1959), p. 48.

1[illegible]. Basically, the work of Terwilliger and Jones[17, 1[illegible]] was concerned with the use of a pulsed localized field bump which served to perturb the entire beam into a region of strong DC magnetic field, whence it would be [illegible]ent down the spiral and out of the accelerator. Terwilliger's investigation[17] of combined radial and axial motion indicated considerable phase distortion (and, effectively, loss of phase density) in the unperturbed accelerator if one employed amplitudes comparable with the stability limits. With a beam for which the oscillation amplitudes specifically were originally about one-half as great as the stability limits, however, so that the coupling was not pronounced, and for which the amplitudes each were further damped [illegible]y a factor of about 7 during the acceleration process, use of the pulsed field was then found to permit orderly extraction with high efficiency.

20. The chief programs employed in this work with the MURA IBM-704 computer were the following:

(a) Snyder, J. N. DUCK ANSWER (Program 75). Midwestern Universities Research Association report MURA-237, Madison, 1957;

(b) Storm, M. R. DUCK WADDLE (Program 249). Midwestern Universities Research Association report MURA-476, Madison, 1959;

(c) King, Richard. FORERUNNER (Program 57). Midwestern Universities Research Association report MURA-240, Madison, 1957;

(d) Chapman, Elizabeth Z. ILL TEMPERED FIVE (Program 220). Midwestern Universities Research Association report MURA-457, Madison, 1959

CAPTIONS FOR FIGURES

Fig. 1. Phase plot, for $s = 0$ (mod. π), of solutions to Eqn. (5) with $\nu_r/N = 0.3$ and $B = 1.15$.

Fig. 2. Phase plot, for $s = 0$ (mod. 3π), of solutions to Eqn. (6) with $\nu_r/N = 0.3$, $B = 1.15$, and $\lambda = 0.006$. The curves through the upper and lower fixed points are seen to "open up" in the neighborheed of the unstable fixed point situated at $v = -0.44345$, the stable region (shaded) has become smaller than for $\lambda = 0$ (Fig. 1), and the stable fixed point has shifted to $v = -0.0838$. The heavy arrow at A suggests a region from which injected particles would flow to flood the boundaries of the stable region.

Fig. 3. Phase plot of solutions to Eqn. (6), with the same values for the coefficients as were used in Fig. 2 but pertaining to solutions at $s = \pi/2$ (mod. 3π).

Fig. 4. Coordinates of the stable and unstable fixed points situated on the coordinate axis, for solutions of Eqn. (6) with $\nu_r/N = 0.3$, $B = 1.15$, $s = 0$ (mod. 3π) vs. λ. These two fixed points are seen to approach one another as the strength of the perturbation is increased, becoming coincident when λ assumes the critical value $\lambda_c = 0.01136$.

Fig. 5. Phase plot, for $s = 0$ (mod. 3π), of solutions to Eqn. (6) with $\nu_r/N = 0.3$ and $B = 1.15$ when λ has the critical value $\lambda_c = 0.01136$. The point designated F. P. represents the confluent fixed point.

Figs. 6-11 Evolution of phase plots, similar to Fig. 2, of solutions to Eqn. (6) [with $\nu_r/N = 0.3$, $B = 1.15$, and $\lambda = 0.006$] as the reference point is

successively taken at $s = 0, \pi/2, \pi, 3\pi/2, 2\pi$, and $5\pi/2$ (mod. 3π). Corresponding points in this set of diagrams are denoted by the letters A, B, ... H.

Fig. 12. Range of initial momenta, p_{v_0}, vs. the initial value, λ_0, of λ, for capture of particles into the stable area of Fig. 1 when the initial coordinate is $v_0 = -0.55$. The results were obtained computationally for solutions of Eqn. (6) with the perturbation decreased to zero at the rate $\frac{d\lambda}{ds} = -\frac{0.002}{3\pi}$.

Fig. 13. Range of initial conditions for capture of particles into the stable area of Fig. 1 when the initial strength of the perturbation is $\lambda_0 = 0.0165$ and $\frac{d\lambda}{ds} = -\frac{0.002}{3\pi}$. The boundary ab transforms, after three sectors ($\Delta s = 3\pi$), to $v = -0.55$.

Fig. 14. Detailed portion of diagram, similar to Fig. 13, for capture of particles with $\lambda_0 = 0.0195$. Particles with initial values represented by circles are captured and those depicted by the crosses are not. The points denoted by c and d represent initial values which were found to lead to stable motion and thus provide evidence of an apparant incipient filamentation (see footnote, p. 15 of text).

Fig. 15. Area of phase space from which particles may be successfully injected into the stable area of Fig. 1, as a function of λ_0, for $\frac{d\lambda}{ds} = -\frac{0.002}{3\pi}$. The ordinates were obtained from diagrams of the type illustrated in Fig. 13, in which one boundary represents the locus of points which transform after three sectors to $v = -0.55$. From the data shown here, the result $\int A(\lambda)\, d\lambda = 0.00046$ was obtained.

Fig. 16. Transformation of the shaded area depicted in Fig. 13 from $s = 0$ to $= \pi/32$, so that this region becomes more centrally located with respect to $p_v = 0$ (compare Figs. 2 and 3, for which the corresponding values of s differ by $\pi/2$). The segment a'b' of the boundary represents the transformation of the portion denoted as ab on Fig. 13. In either case the shaded region has an area estimated as 0.042 $v \cdot p_v$-units.

Fig. 17. Phase plots at $s = 3\pi/32$, mod. π, for $\lambda = 0$.

Fig. 18. Phase plots at $s = 3\pi/32$, mod. 3π, for $\lambda = 0.006$.

Fig. 19. Phase plots at $s = \pi/2$, mod. π, for $\lambda = 0$.

Fig. 20. Phase plots at $s = \pi/2$, mod. 3π, for $\lambda = 0.006$.

Figs. 21-30. Range of initial conditions for capture into the stable area when $s = 3\pi/32$ and the initial strength of the perturbation (at $s = 3\pi/32$) is, respectively, 0.0054375, 0.0074375, ... 0.0234375.

Fig. 31. Range of initial conditions for capture into the stable area when $s = 3\pi/32$ and the initial strength of the perturbation is $\lambda = 0.0174375$. This diagram is identical to that shown in Fig. 27, save that the right-hand edge of the area of acceptance has now been located at $v = -0.55$.

Fig. 32. Region of axial phase space leading to an estimated 88% filling of the stable phase volume, if used at $s = 3\pi/32$ with three-sector injection and $d\lambda/ds = -\frac{0.002}{3\pi}$, with $-1.26 \leq v \leq -0.55$ and $-0.21 \leq p_v \leq +0.05$.

Fig. 33. Radial phase plots, pertaining to $33\theta = 0$ (mod. 2π), for a spiral sector accelerator with N = 33, k = 79, 1/w = 1252, and $f = \frac{1}{4}$ The rotation number becomes close to $2\pi/3$ for phase trajectories passing close to point C, although no fixed point of order 3 was found. The region

of ra ial phase space of which effective use could be made might be considered to be substantially that contained within the largest full-line curve on this [illegible]

Fig. 34. Radial phase plots, pertaining to $33\theta = 0$ (mod. 6π), for a perturbed spiral sector accelerator for which the parameters are the same as for the [illegible]ucture to which Fig. 33 applies, save for the addition of the field-perturbation $-0.0015 \cos\left\{\frac{1}{3}\left[\frac{1}{\omega}\ln(1+x) - N\theta\right] - \frac{\pi}{4}\right\}$ to $-B_{z,o}/r^k$. The point P denotes an unstable fixed point and the solid curve may be considered to enclose an area which grows as the perturbation decreases in strength and within which particles may be captured.

Fig. 34. Phase diagram intended to explai the occurance of apparent filamentation of phase space destined for capture, in which phase trajectories passing close to the fi d points C and B move sufficiently slowly that the perturbation becomes sufficiently reduced to permit capture of such particles (see footnote, p. 15). The phase-trajectories illustrated originated at $v = -0.95$, with $-0.246 \leq p_v \leq -0.305$, when $\lambda = 0.0195$ (see Fig. 14, esp. insert).

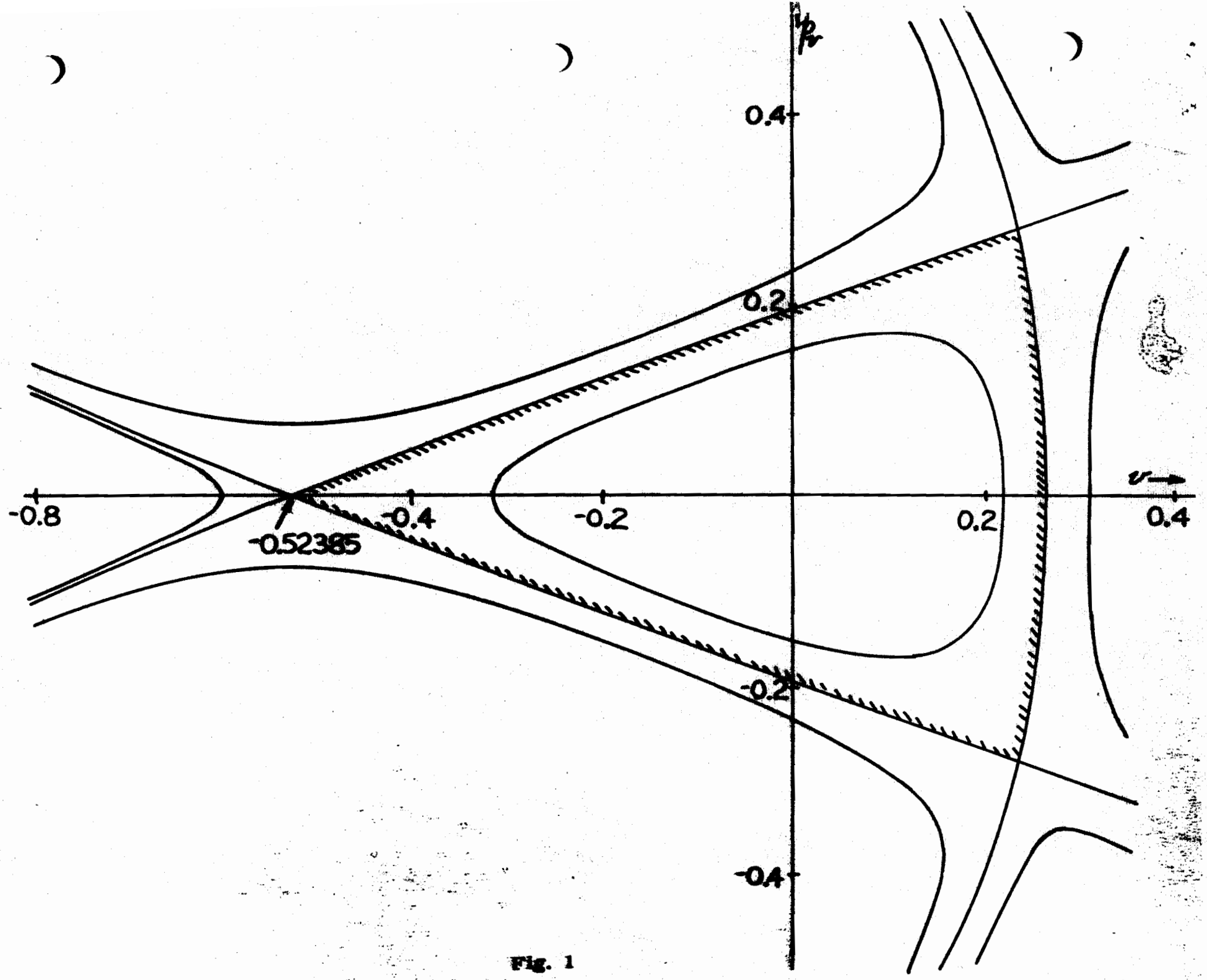

Fig. 1

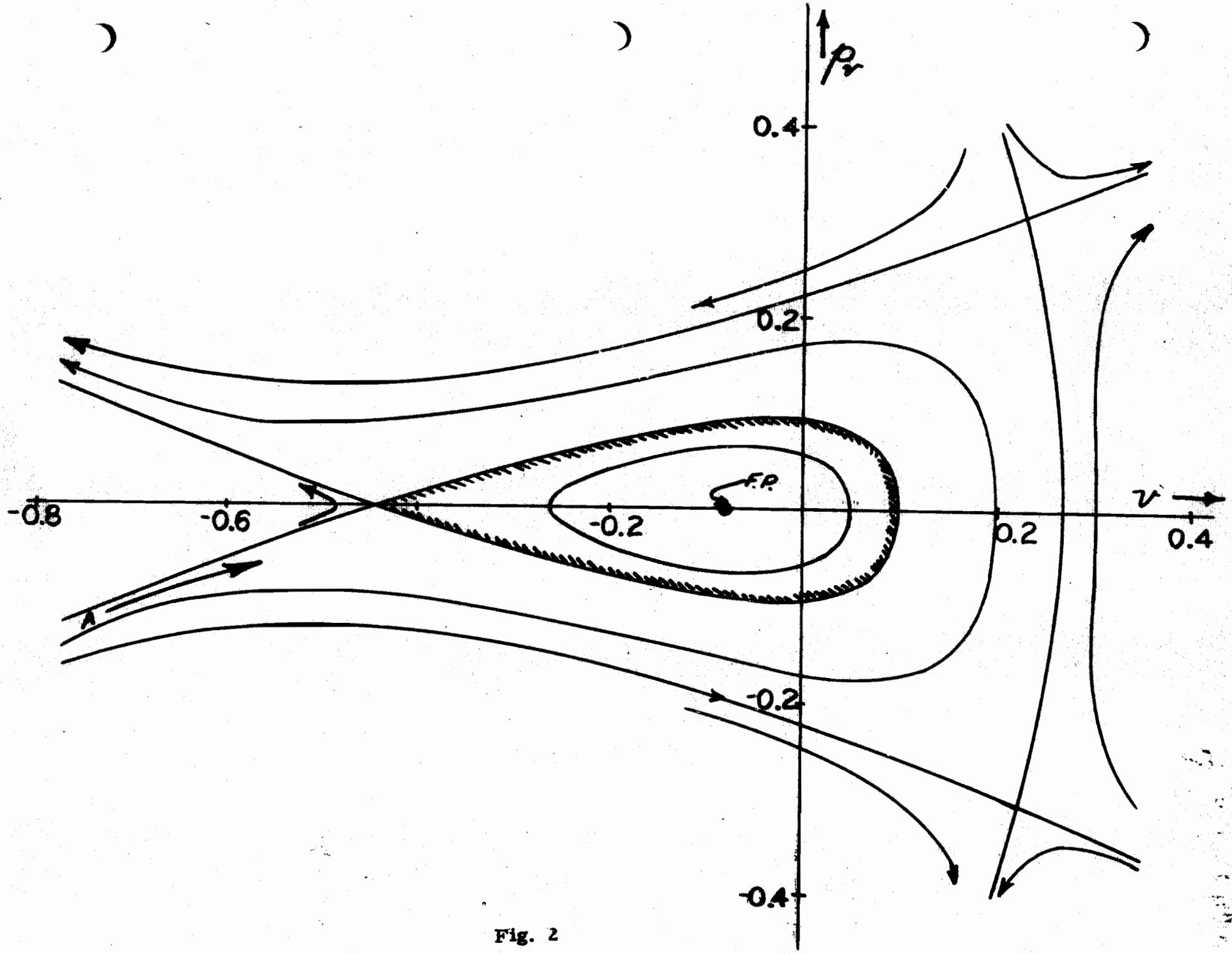

Fig. 2

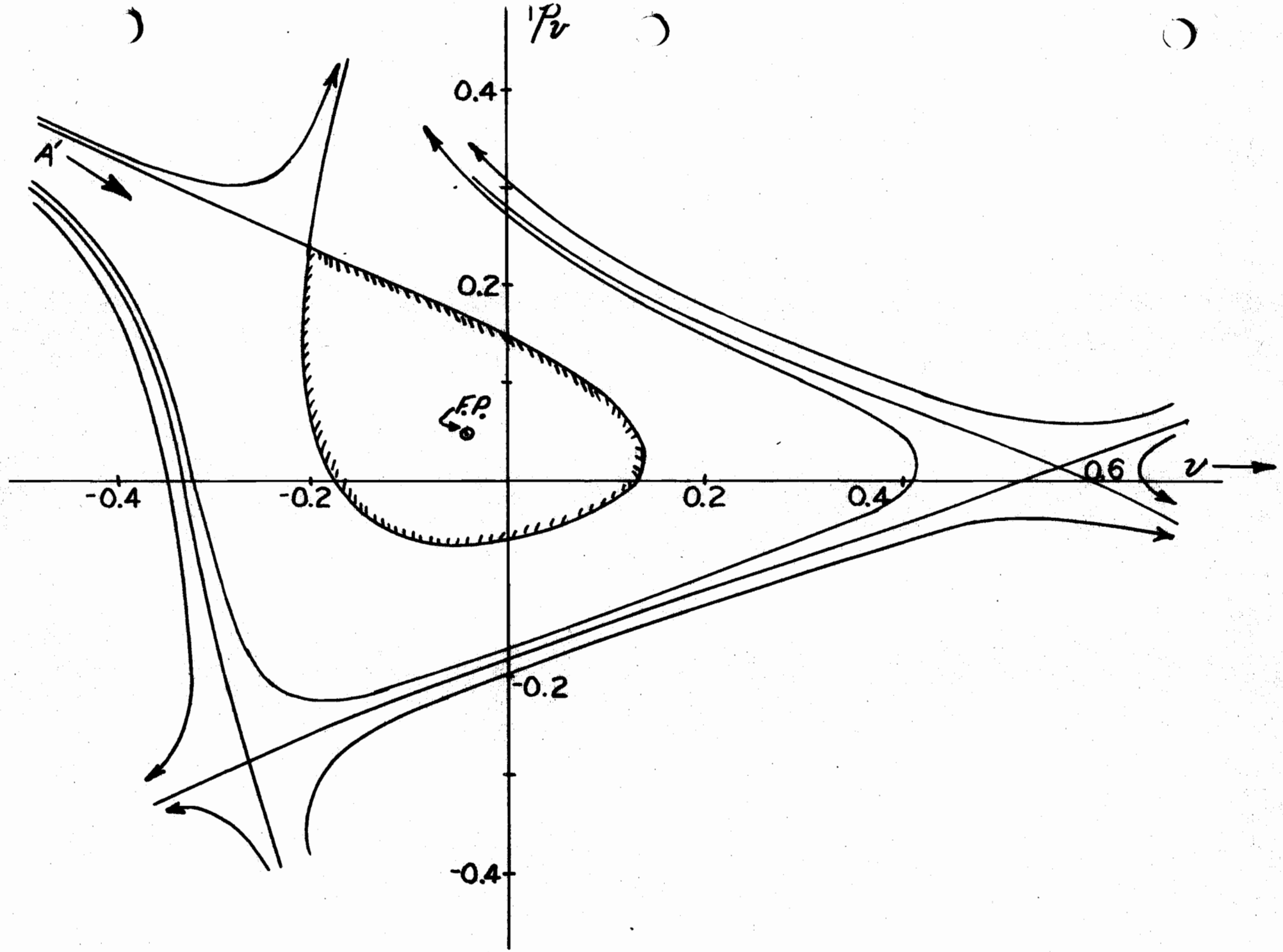

Fig. 3

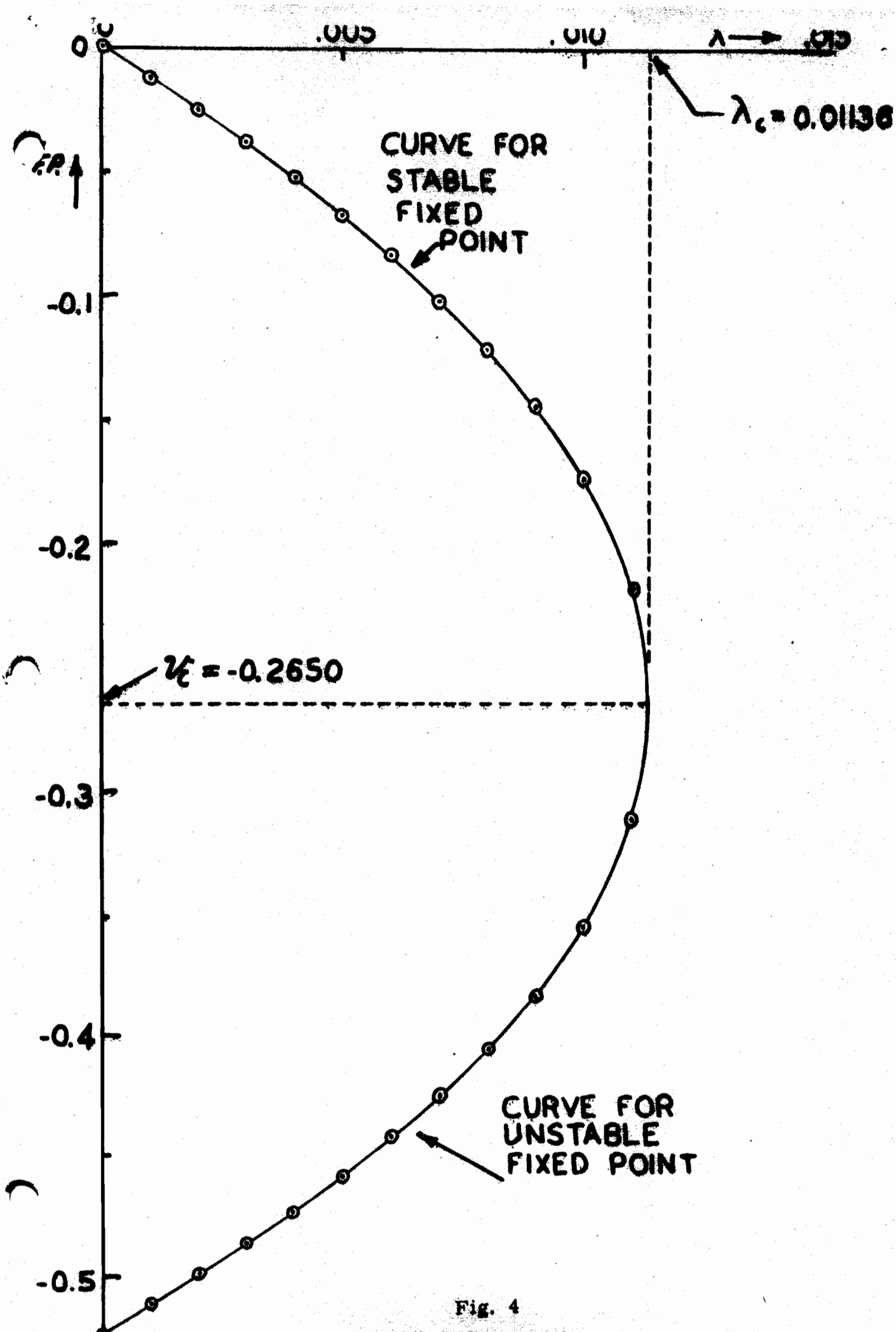
0
.005
.010
λ
$\lambda_c = 0.01136$
CURVE FOR
STABLE
FIXED
POINT
-0.1
-0.2
$\nu_c = -0.2650$
-0.3
-0.4
CURVE FOR
UNSTABLE
FIXED POINT
-0.5

Fig. 4

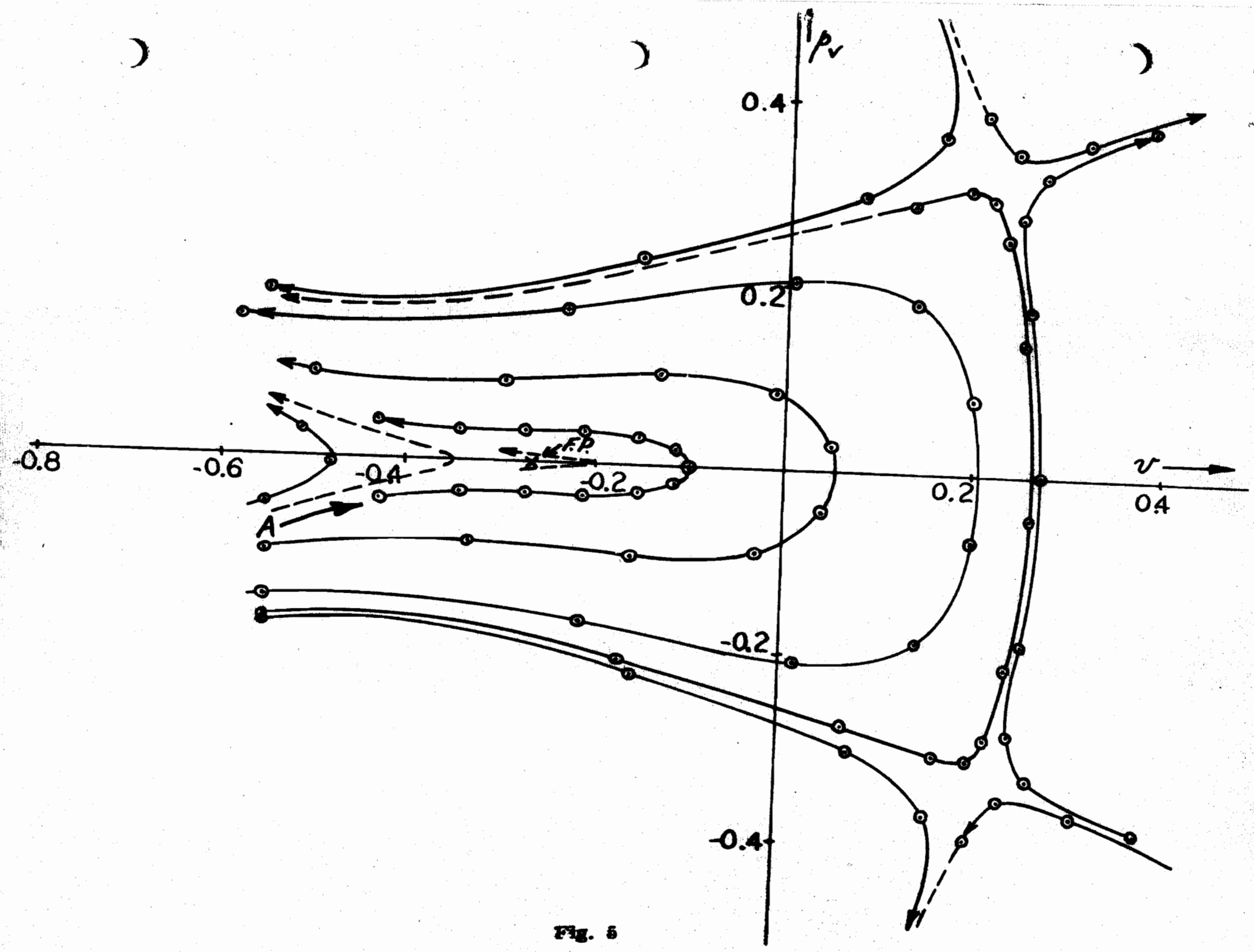

Fig. 5

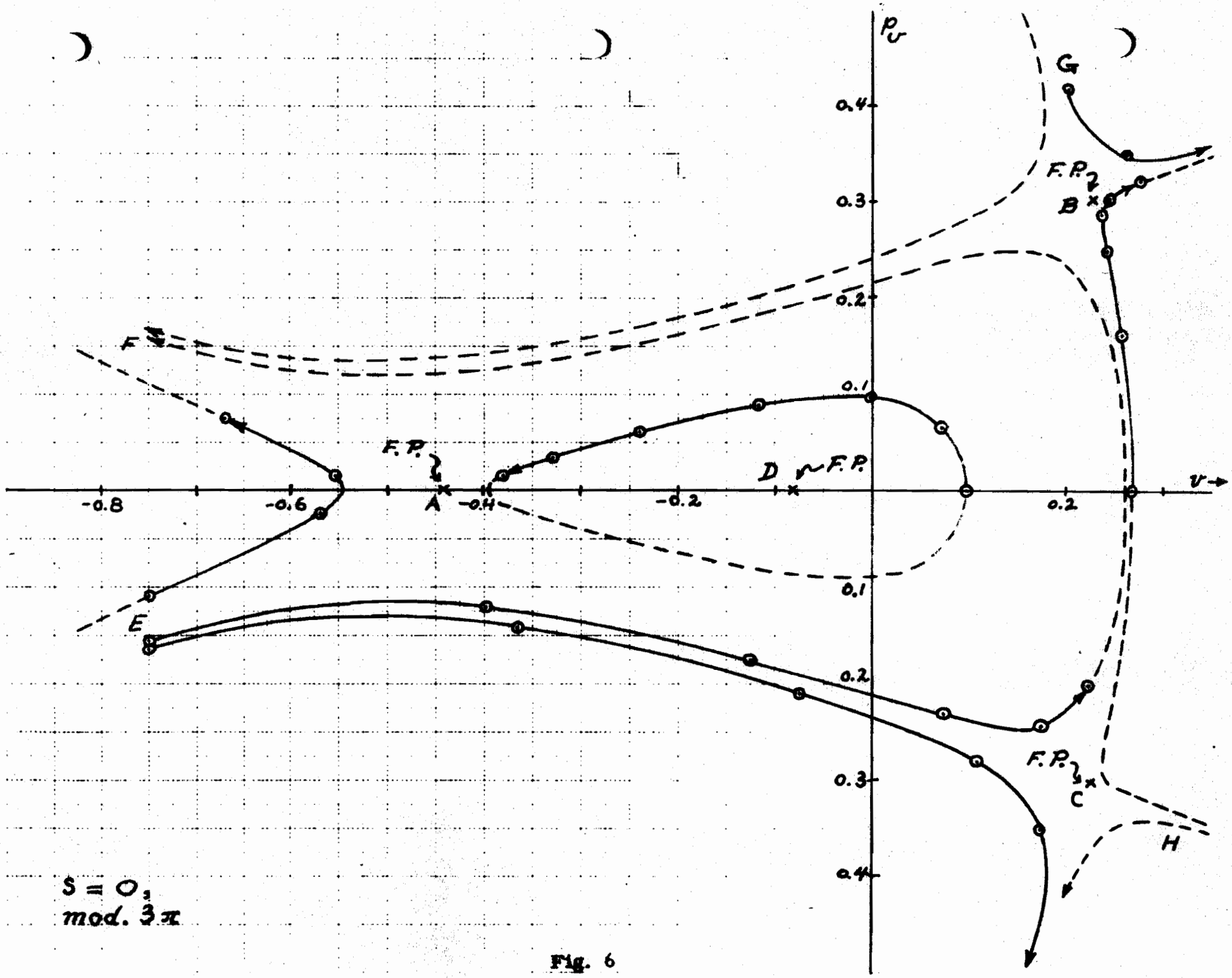
p_v
v
G
F.P.
B
F
F.P.
A
D
F.P.
E
F.P.
C
H
0.4
0.3
0.2
0.1
0.1
0.2
0.3
0.4
-0.8
-0.6
-0.4
-0.2
0.2
$S = 0,$
mod. 3π

Fig. 6

Fig 7

CLEARPRINT PAPER CO. NO. C39X MILLIMETERS 200 BY 250 DIVISIONS
CLEARPRINT CHARTS

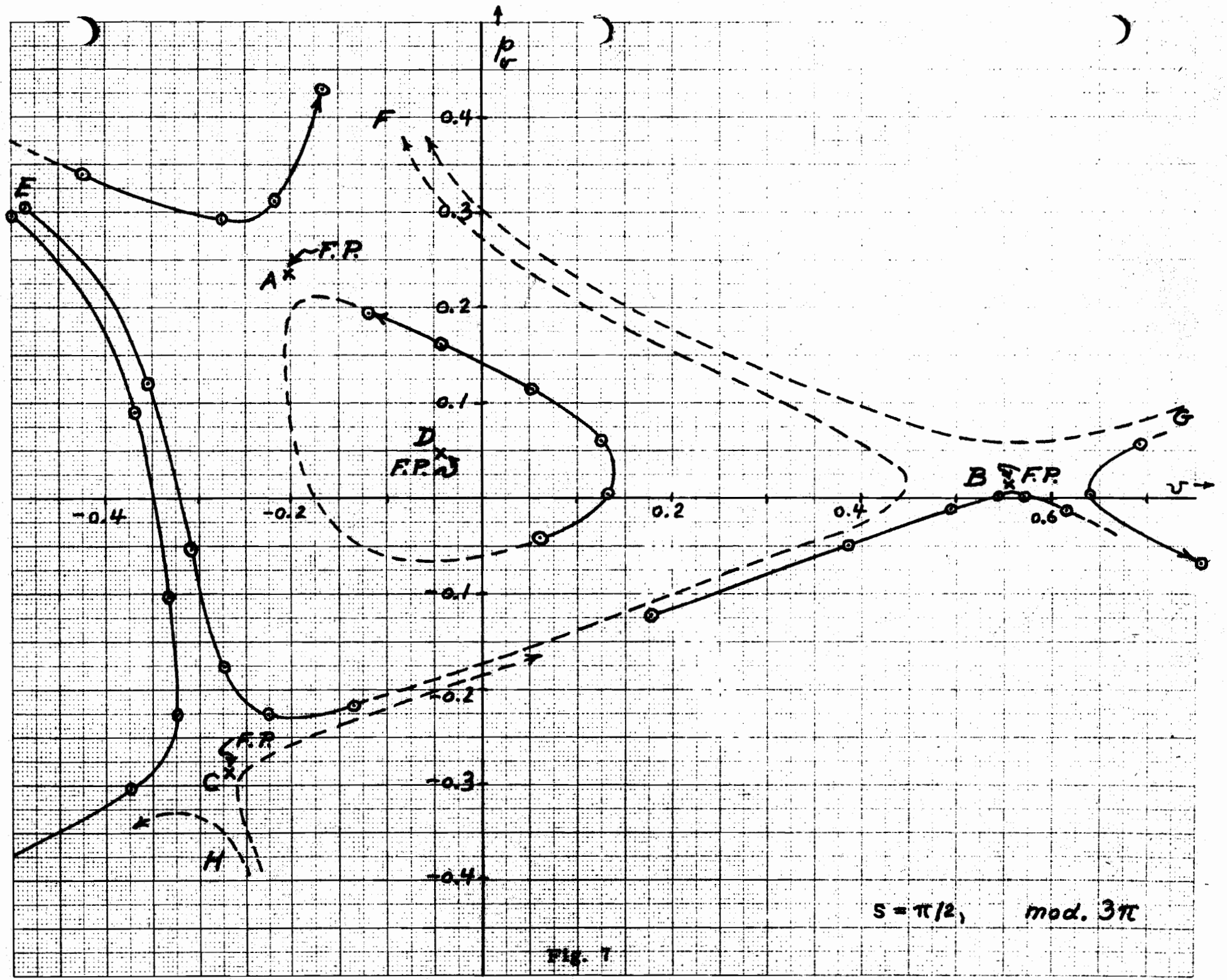

Fig. 7

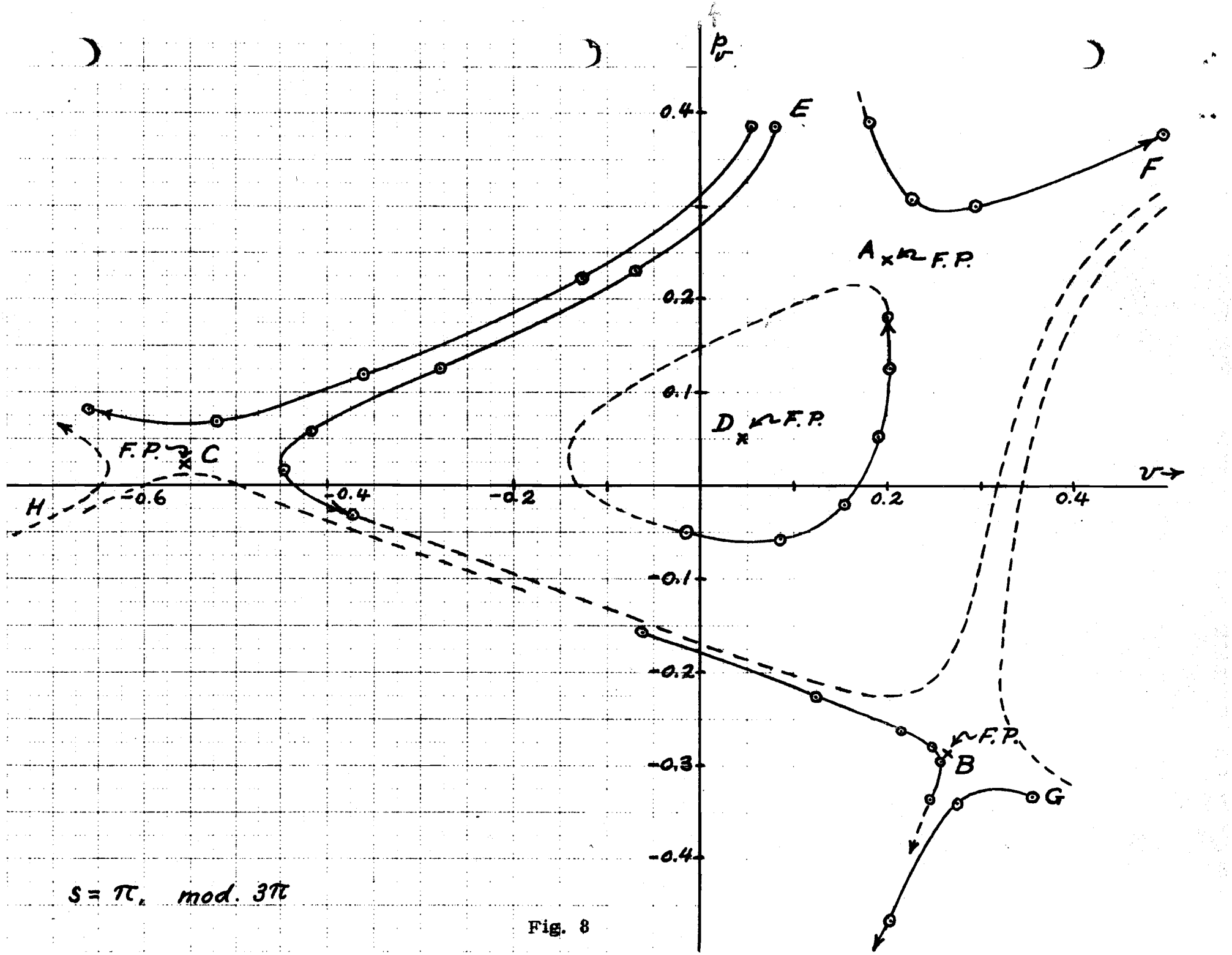
p_v
0.4
0.2
0.1
-0.1
-0.2
-0.3
-0.4
-0.6
-0.4
-0.2
0.2
0.4
$v \rightarrow$
E
F
A
F.P.
D
F.P.
F.P.
C
H
F.P.
B
G
$s = \pi$, mod. 3π

Fig. 8

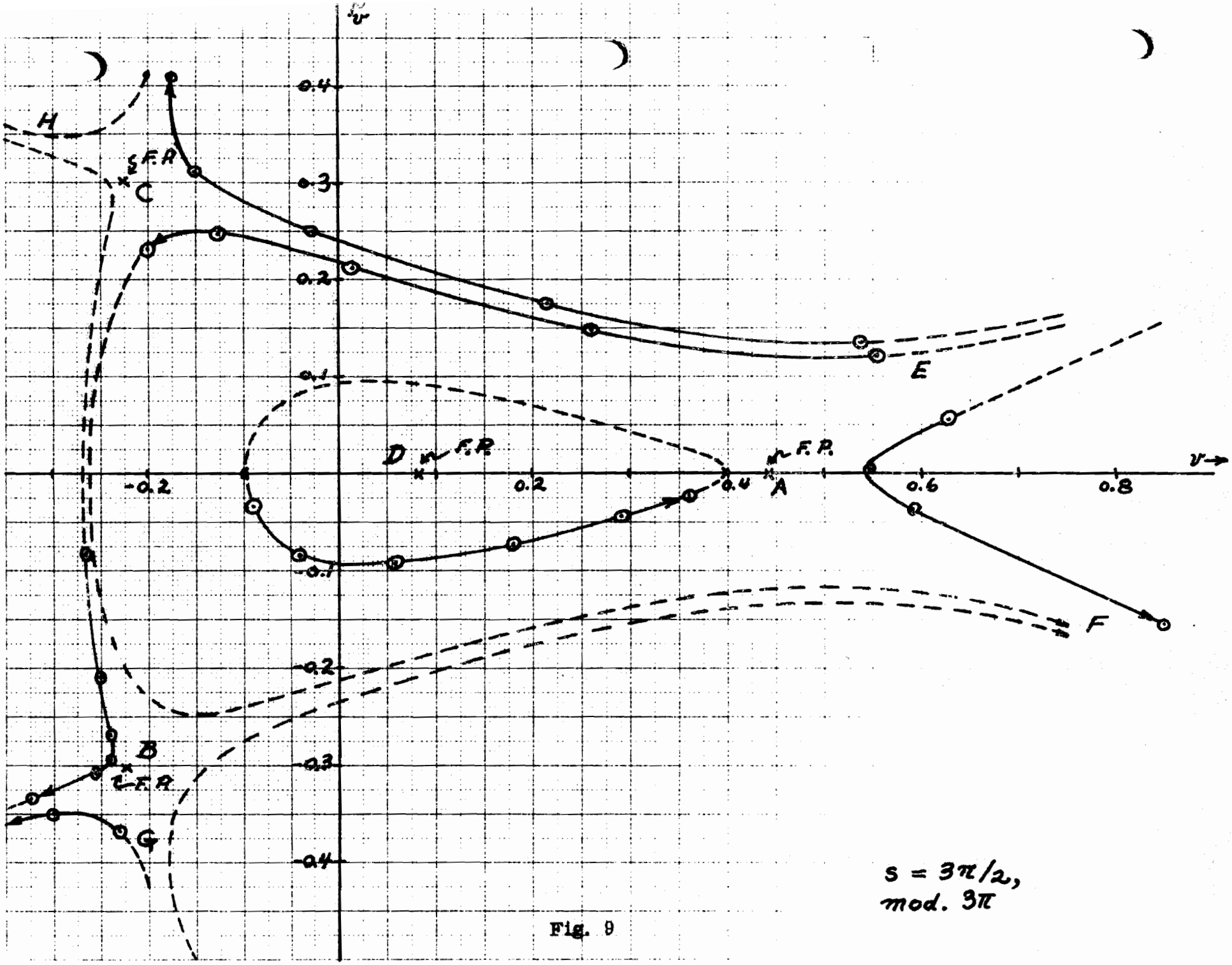

$s = 3\pi/2$,
mod. 3π

Fig. 9

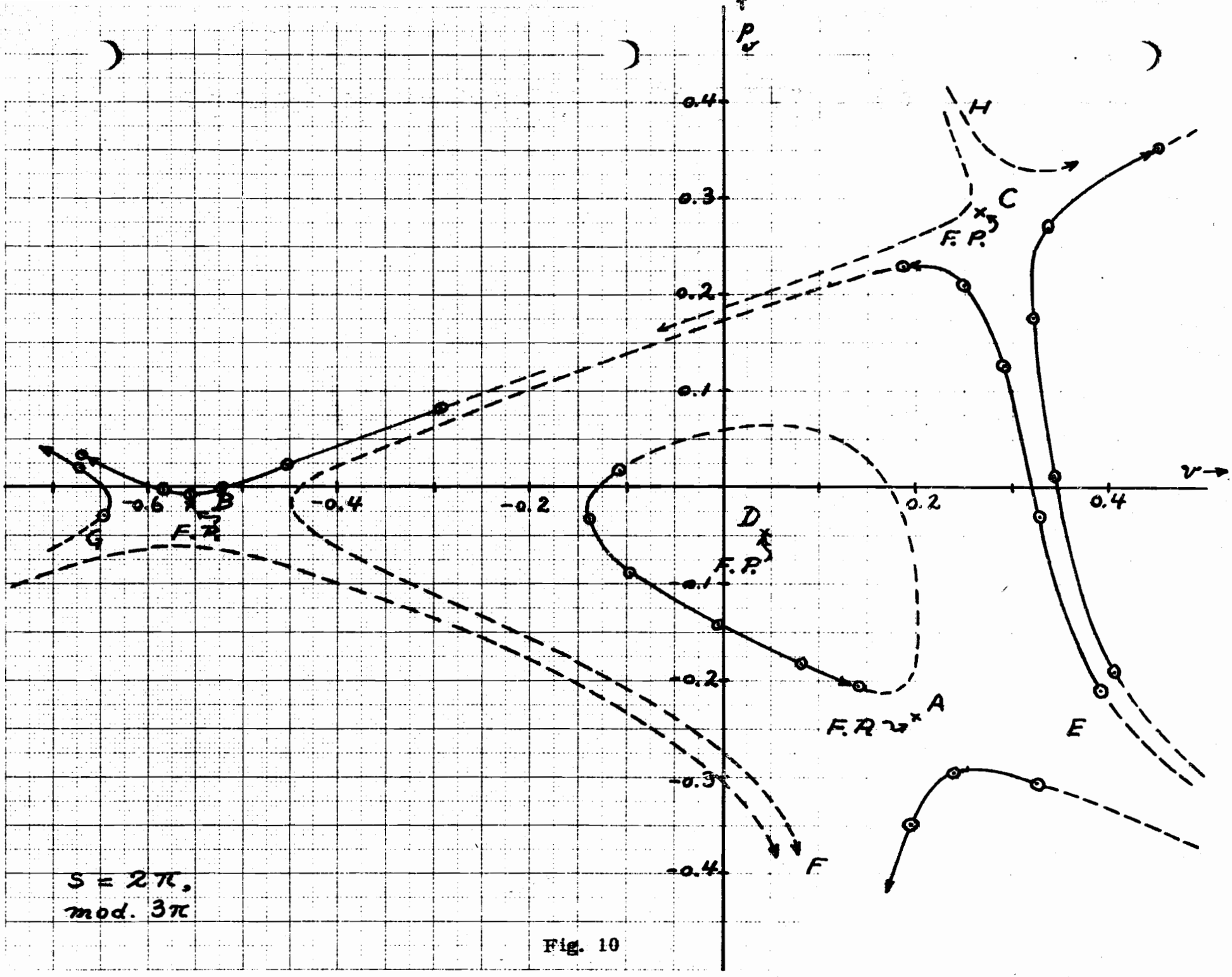
p_v
v
0.4
0.3
0.2
0.1
-0.1
-0.2
-0.3
-0.4
-0.6
-0.4
-0.2
0.2
0.4
H
C
F.P.
B
F.P.
G
D
F.P.
A
F.P.
E
F
$s = 2\pi$,
mod. 3π

Fig. 10

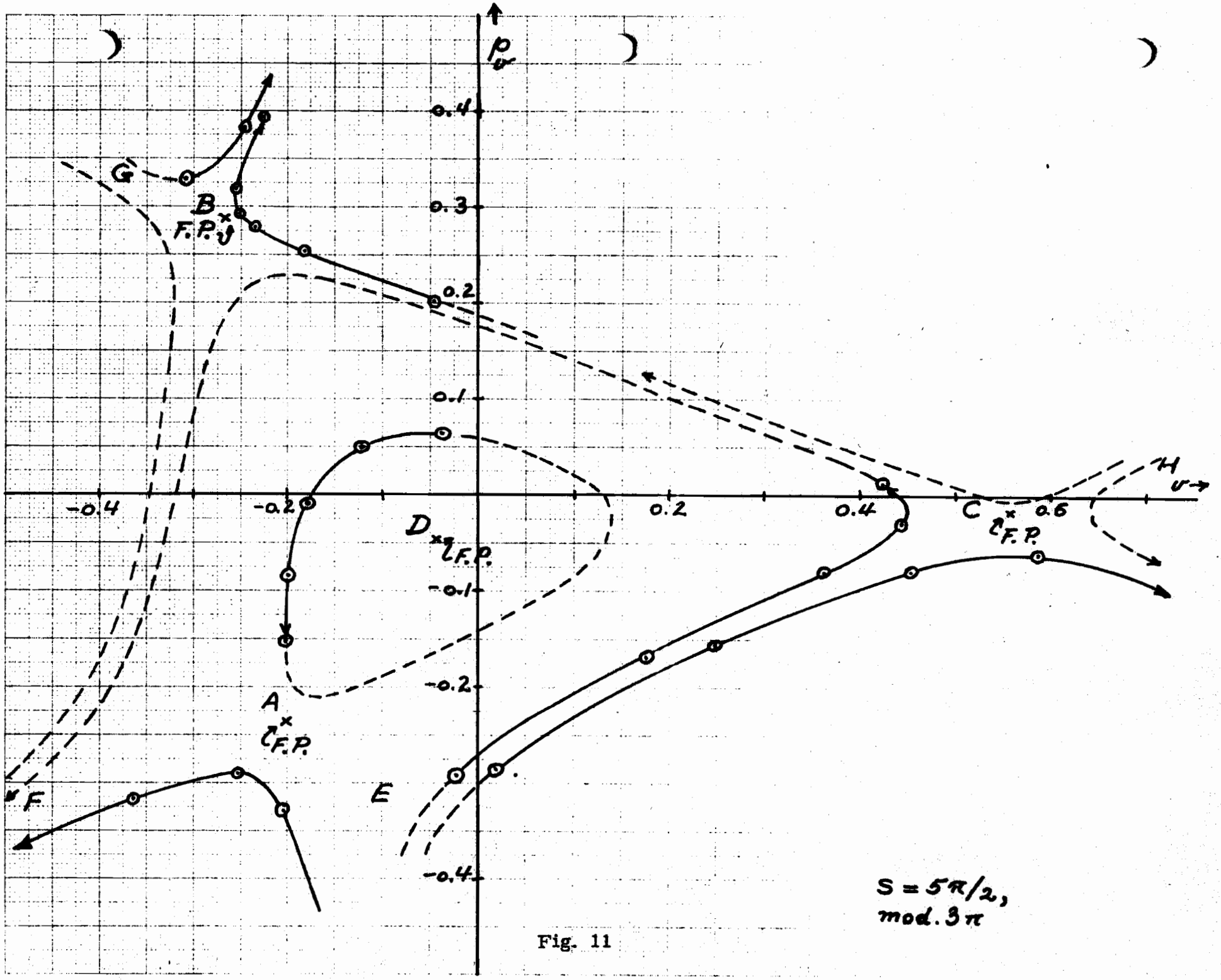

p_v
0.4
0.3
0.2
0.1
-0.1
-0.2
-0.4
-0.4
-0.2
0.2
0.4
0.6
v
G
B
F.P.
D
F.P.
C
F.P.
H
A
F.P.
E
F
S = 5π/2,
mod. 3π

Fig. 11

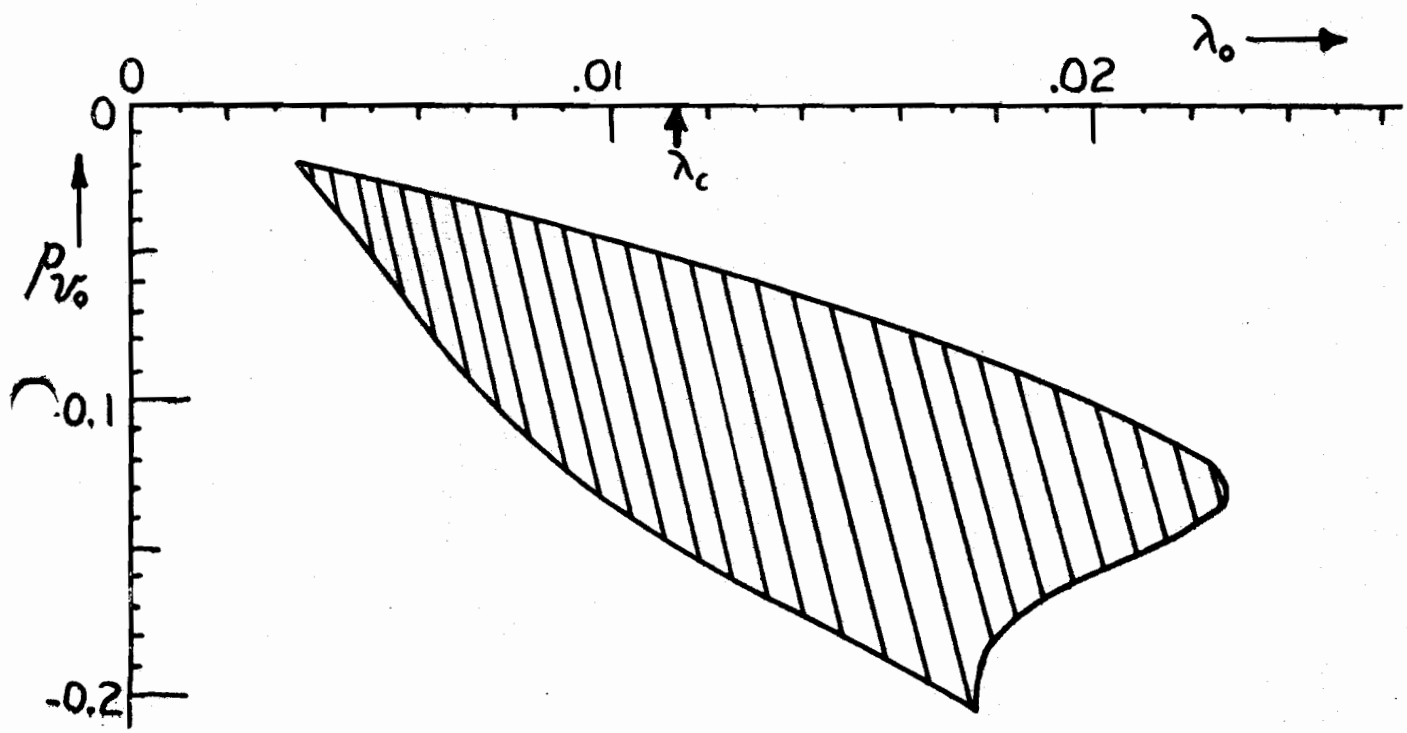

Fig. 12

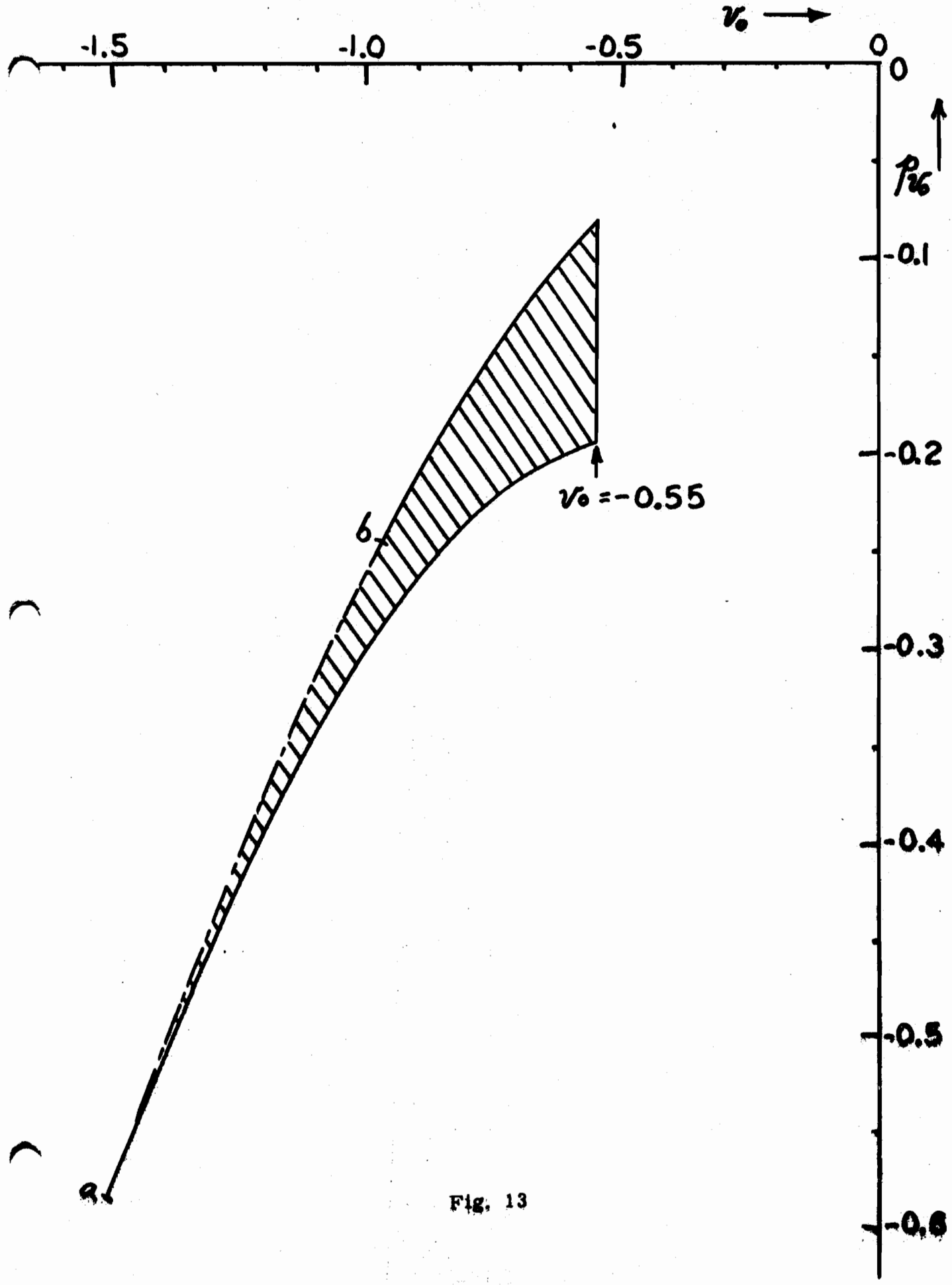

Fig. 13

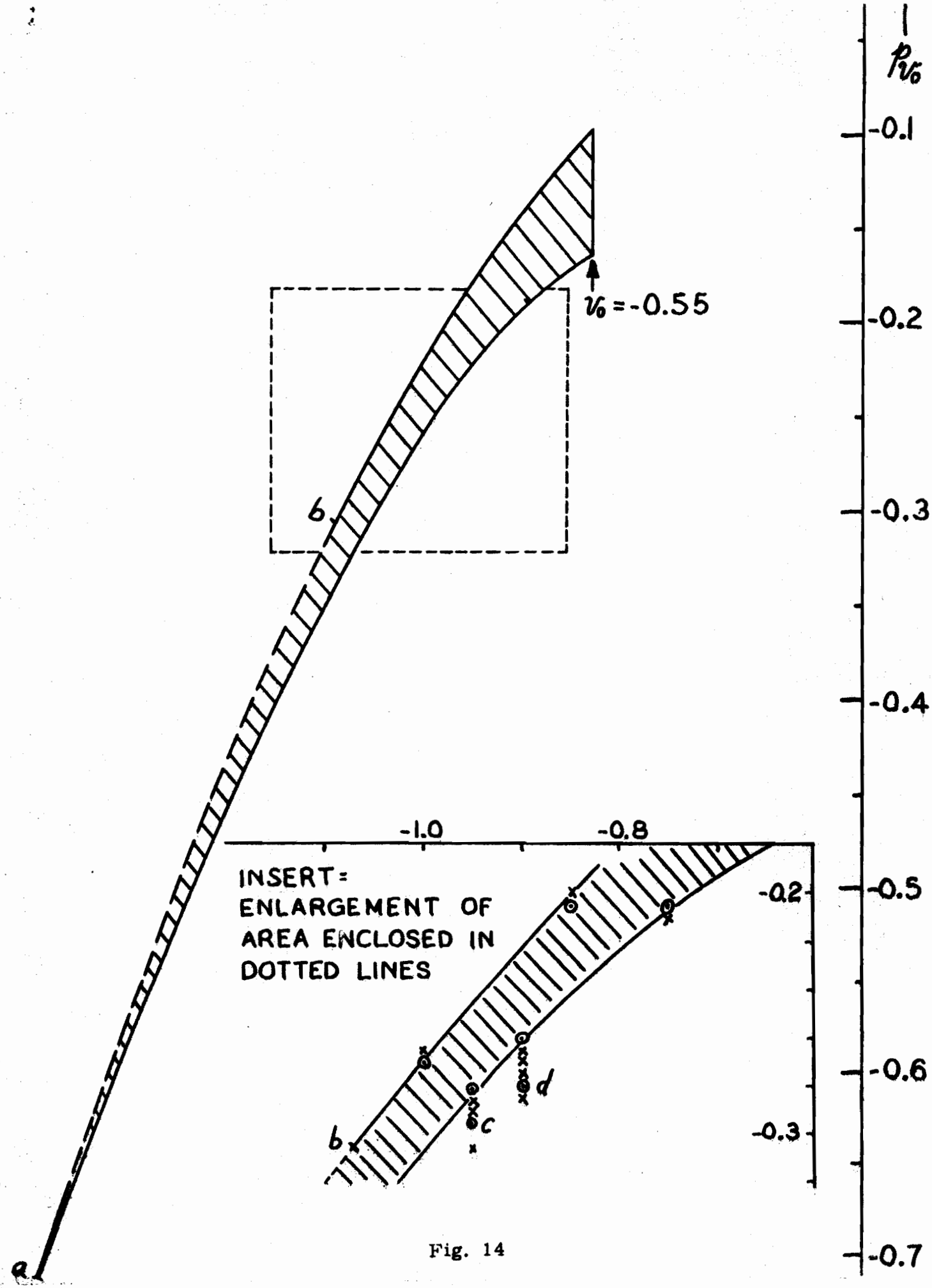
P/V_0
-0.1
-0.2
-0.3
-0.4
-0.5
-0.6
-0.7
$V_0 = -0.55$
a
b
-1.0
-0.8
-0.2
-0.3
INSERT:
ENLARGEMENT OF
AREA ENCLOSED IN
DOTTED LINES
b
c
d

Fig. 14

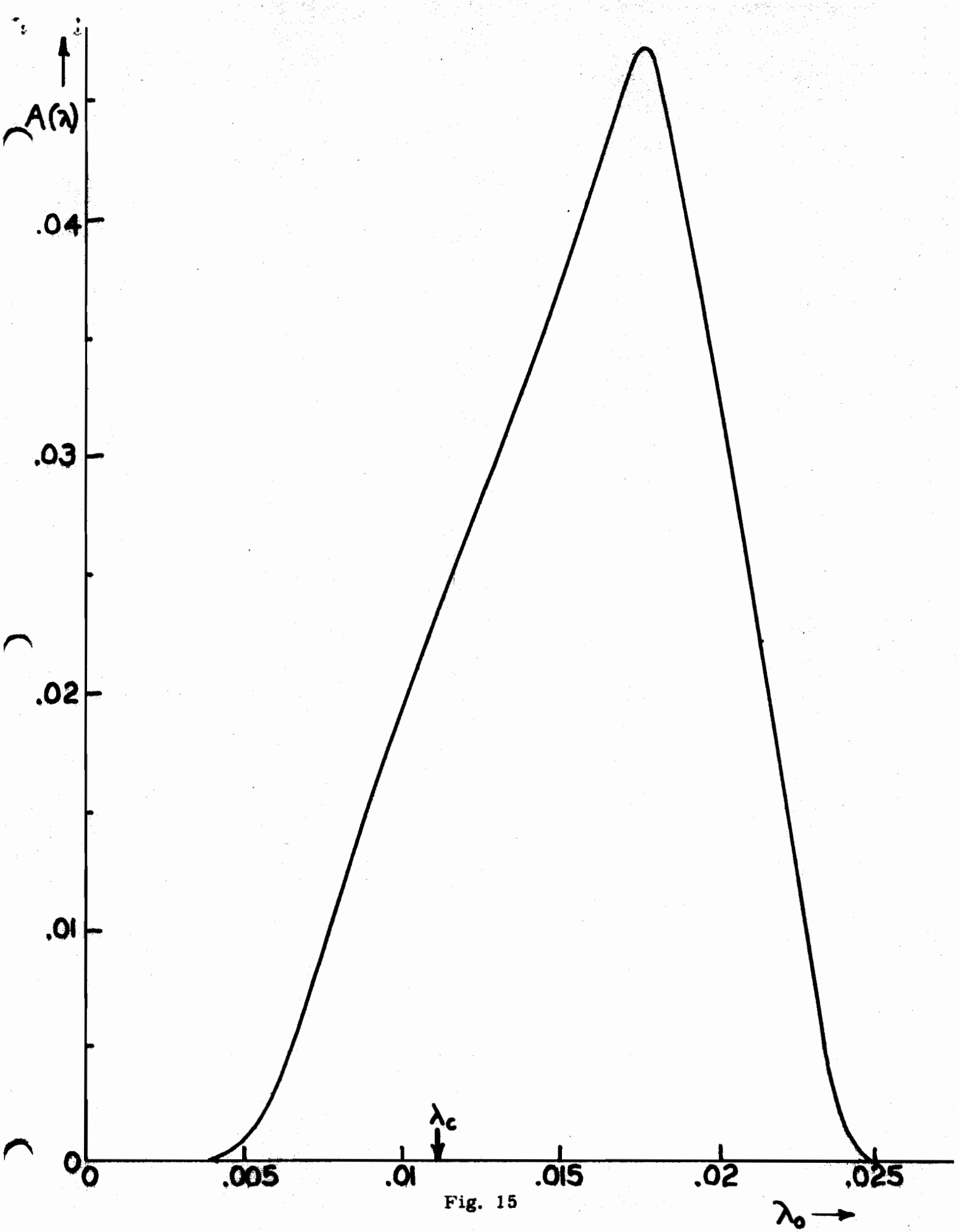

Fig. 15

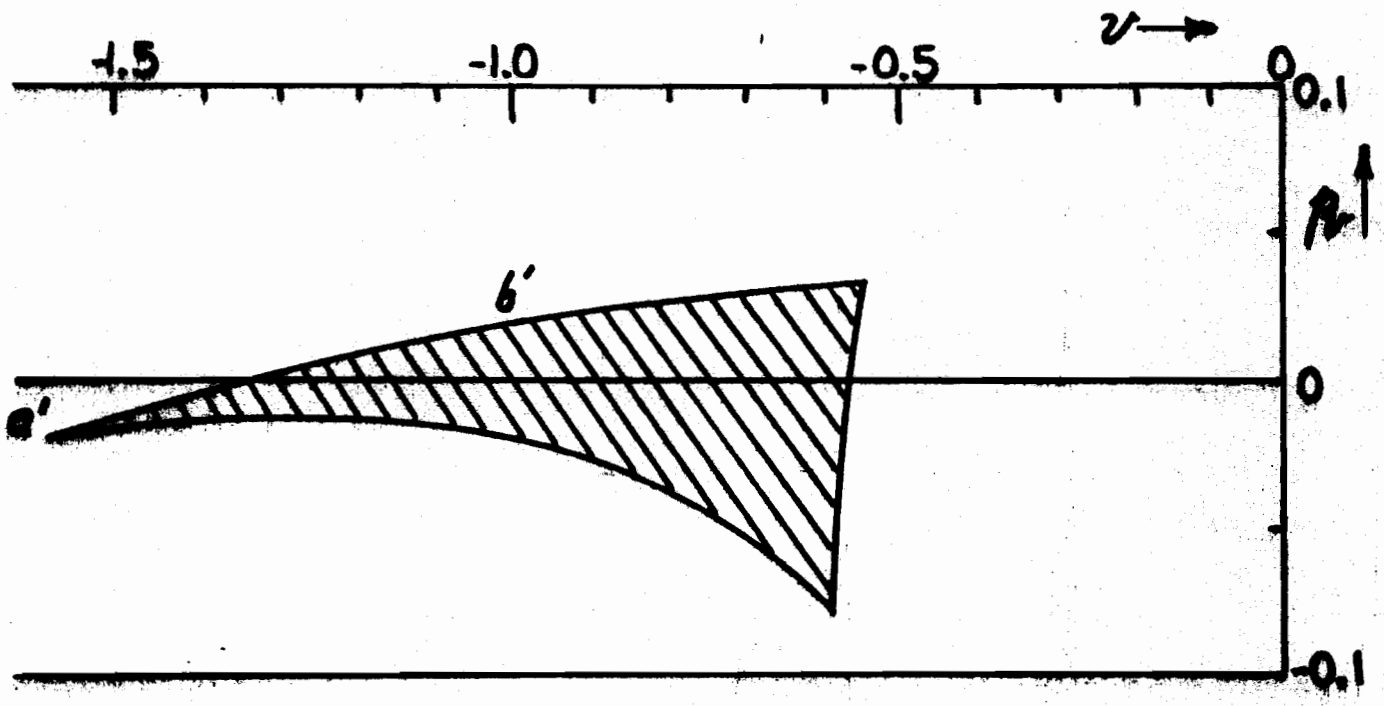

Fig. 16

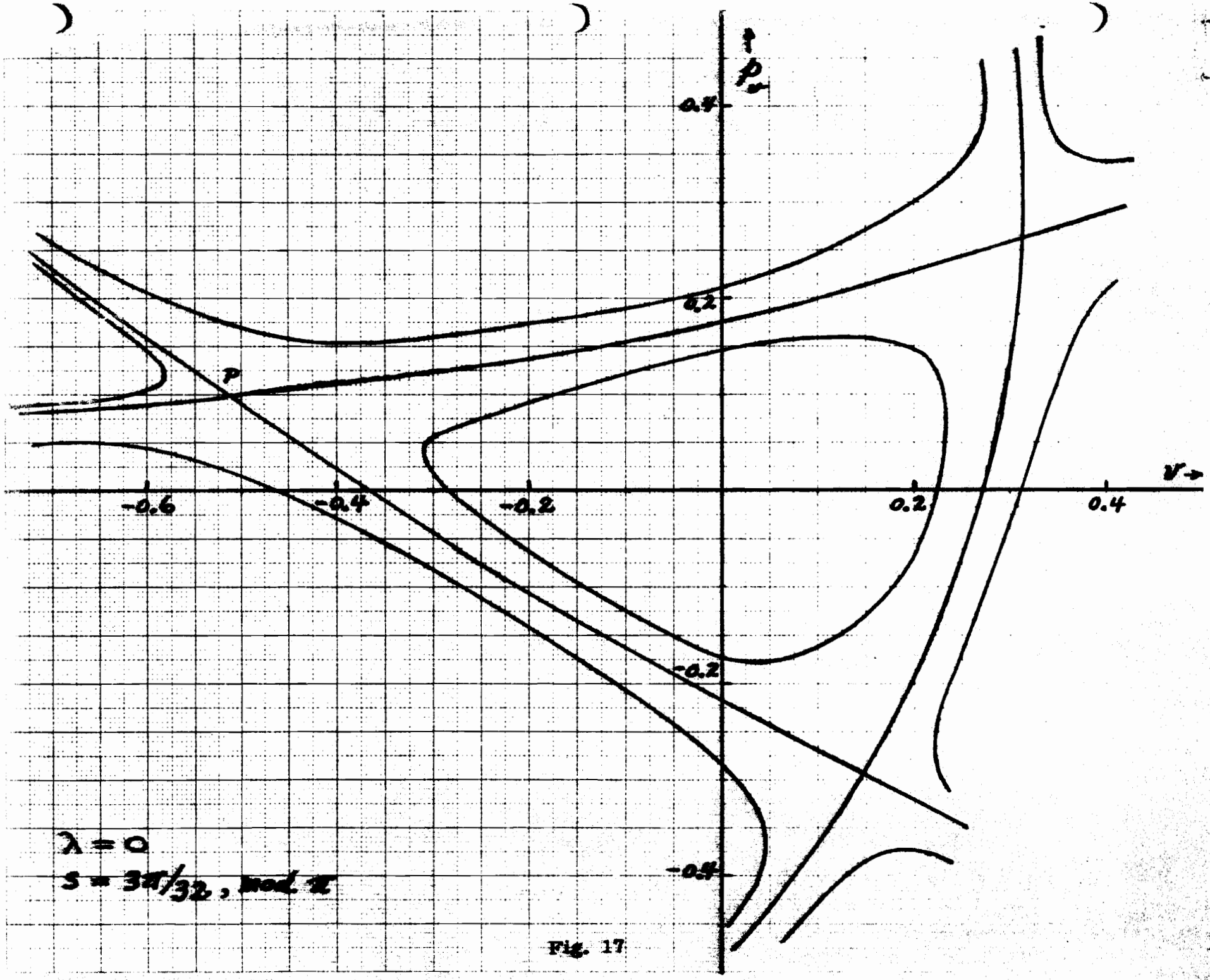
p_v
0.4
0.2
-0.2
-0.4
$v \rightarrow$
-0.6
-0.4
-0.2
0.2
0.4
P
$\lambda = 0$
$s = 3\pi/32$, mod π

Fig. 17

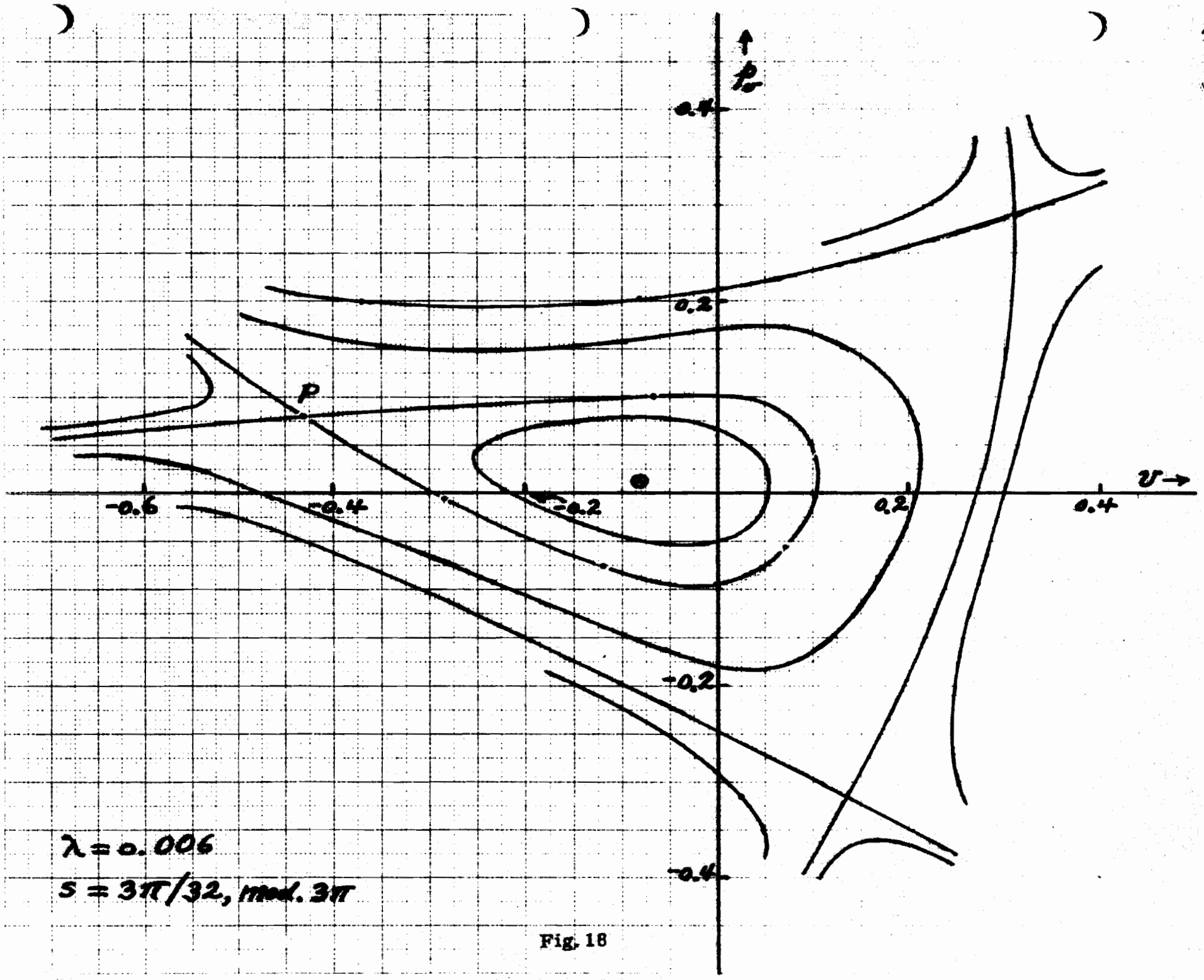

Fig. 18

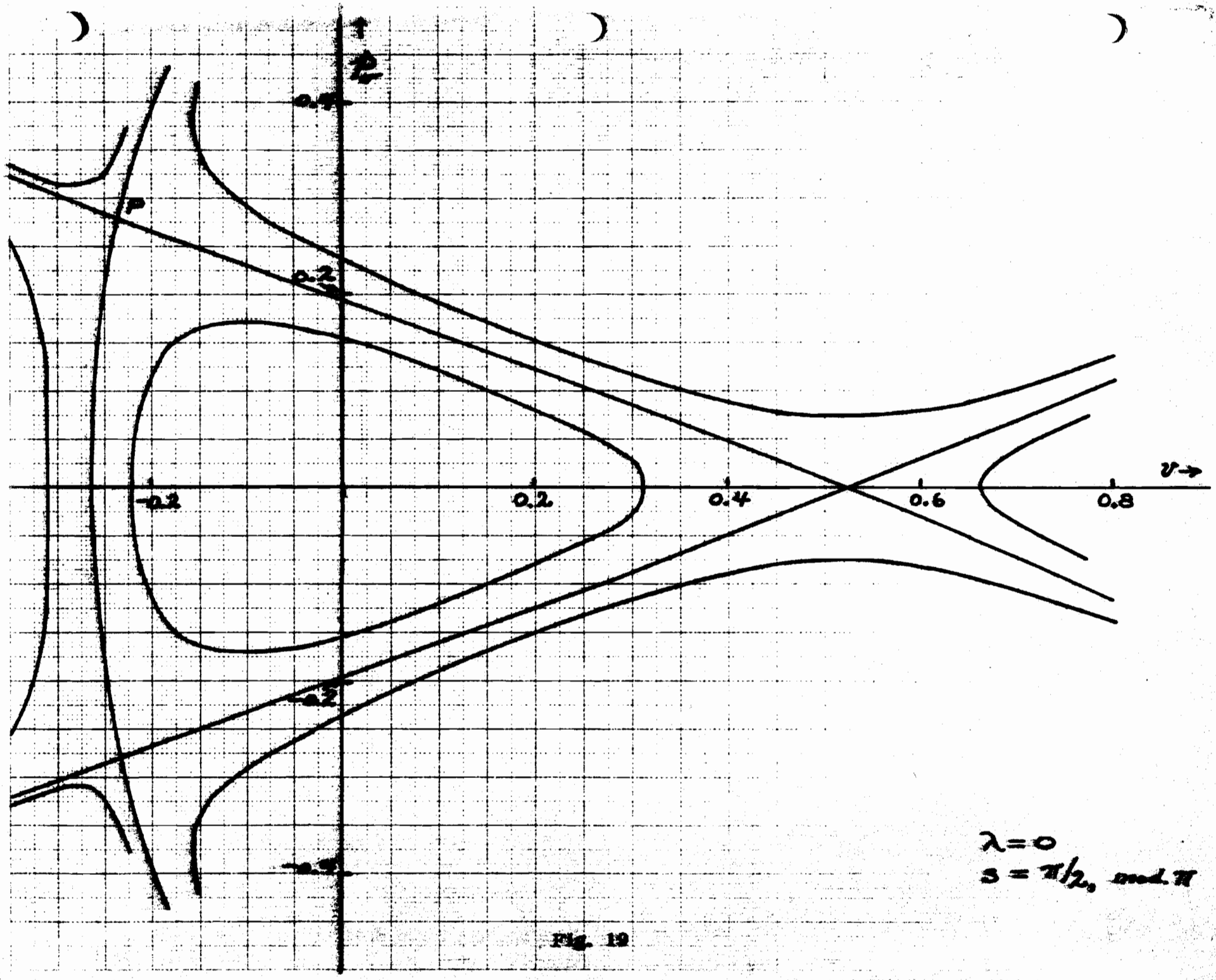

Fig. 19

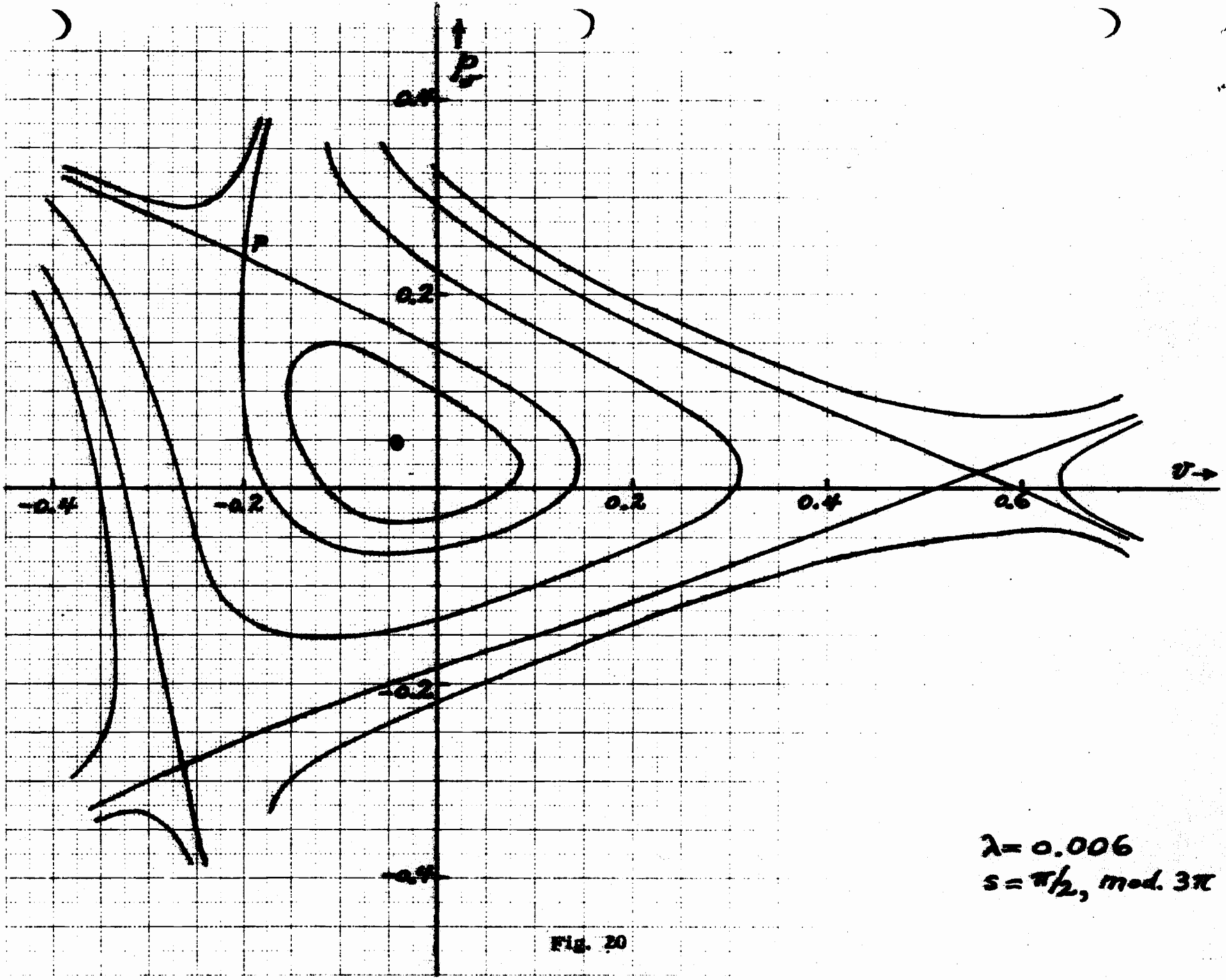
p_v
0.4
0.2
-0.2
-0.4
-0.4
-0.2
0.2
0.4
0.6
$v \rightarrow$
P
$\lambda = 0.006$
$s = \pi/2$, mod. 3π

Fig. 20

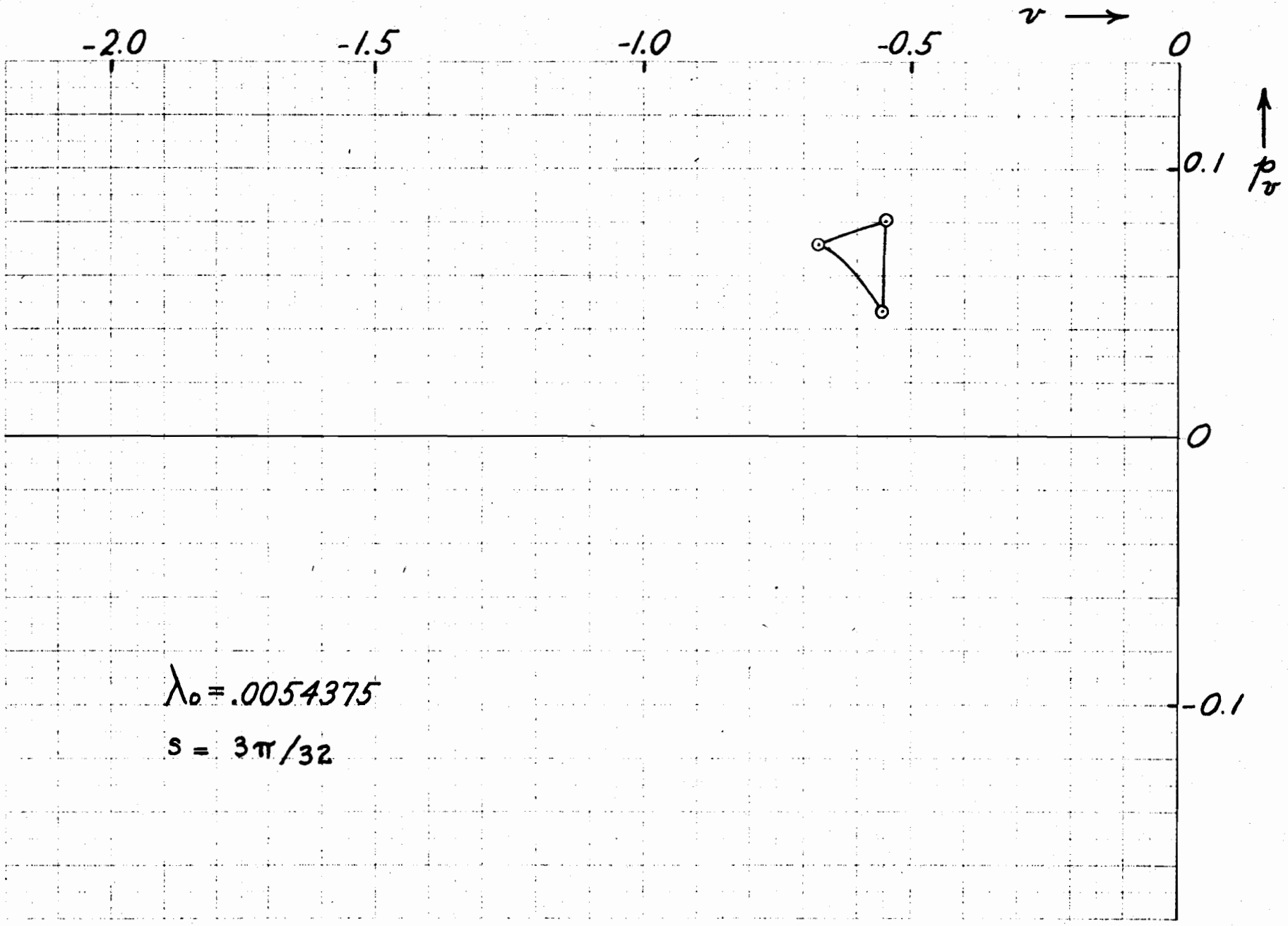

Fig. 21

CLEARPRINT PAPER CO. NO. C29 MILLIMETERS BOTH WAYS 10 X 220 DIVISIONS
CLEARPRINT CHARTS
PRINTED IN U.S.A. ON CLEARPRINT TECHNICAL PAPER NO. 1000H

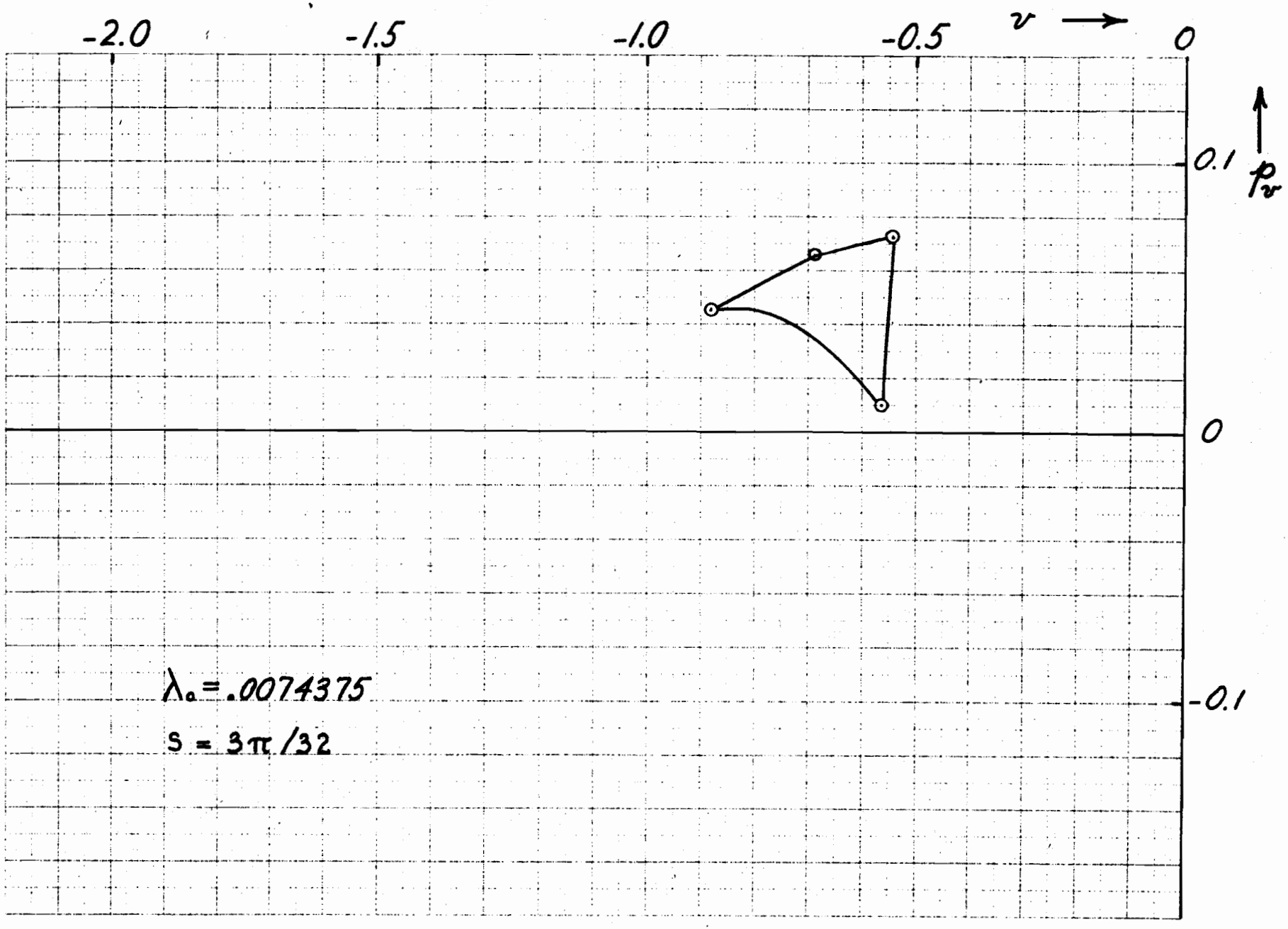

Fig. 22

CLEARPRINT PAPER CO. NO. C39 MILLIMETERS BOTH WAYS 160 X 220 DIVISIONS. PRINTED IN U.S.A. ON CLEARPRINT TECHNICAL PAPER NO. 1000H

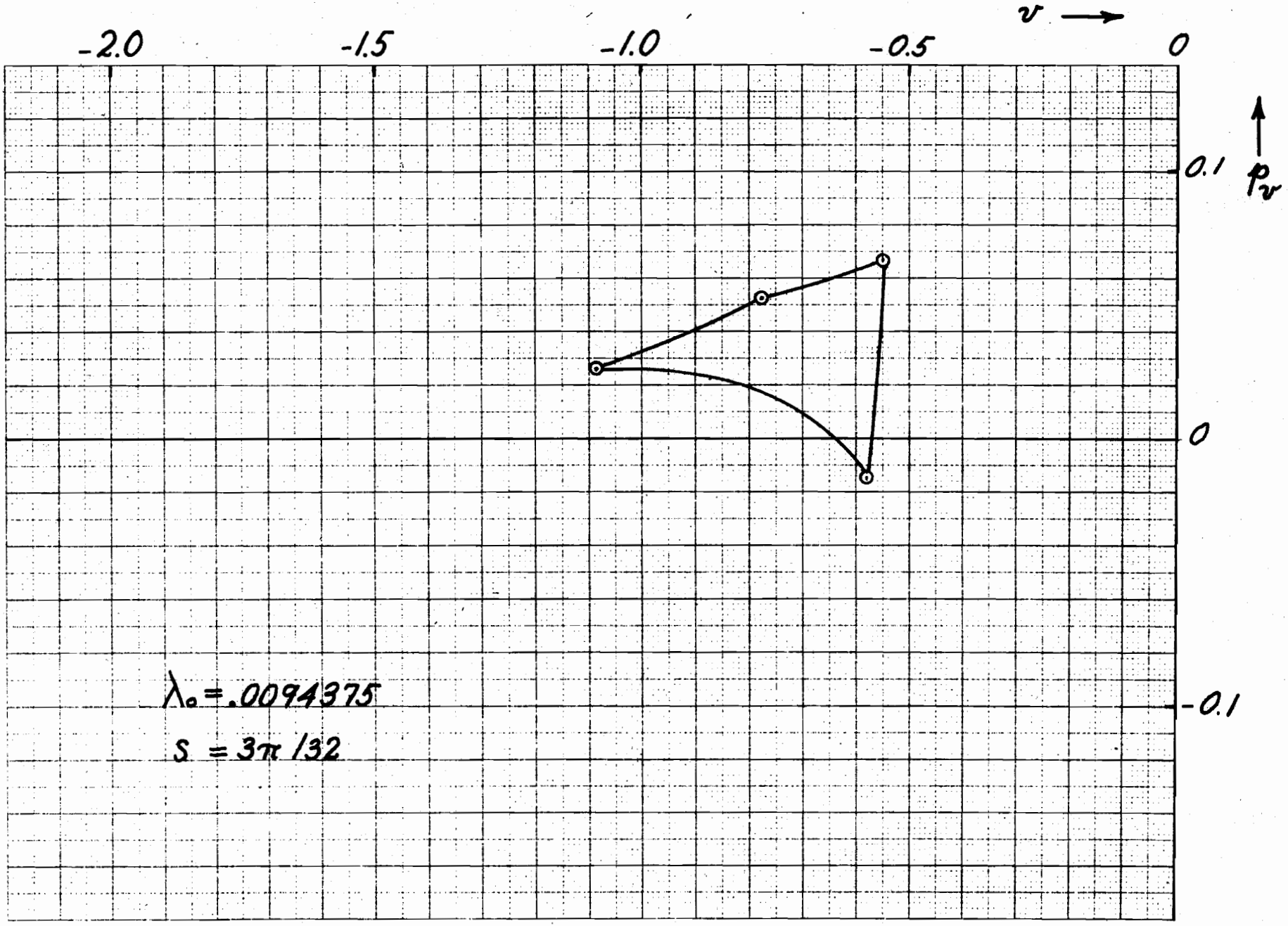

Fig. 23

CLEARPRINT PAPER CO. NO. C39 MILLIMETERS BOTH WAYS 160 X 220 DIVISIONS. CLEARPRINT CHARTS PRINTED IN U.S.A. ON CLEARPRINT TECHNICAL PAPER NO. 1000H

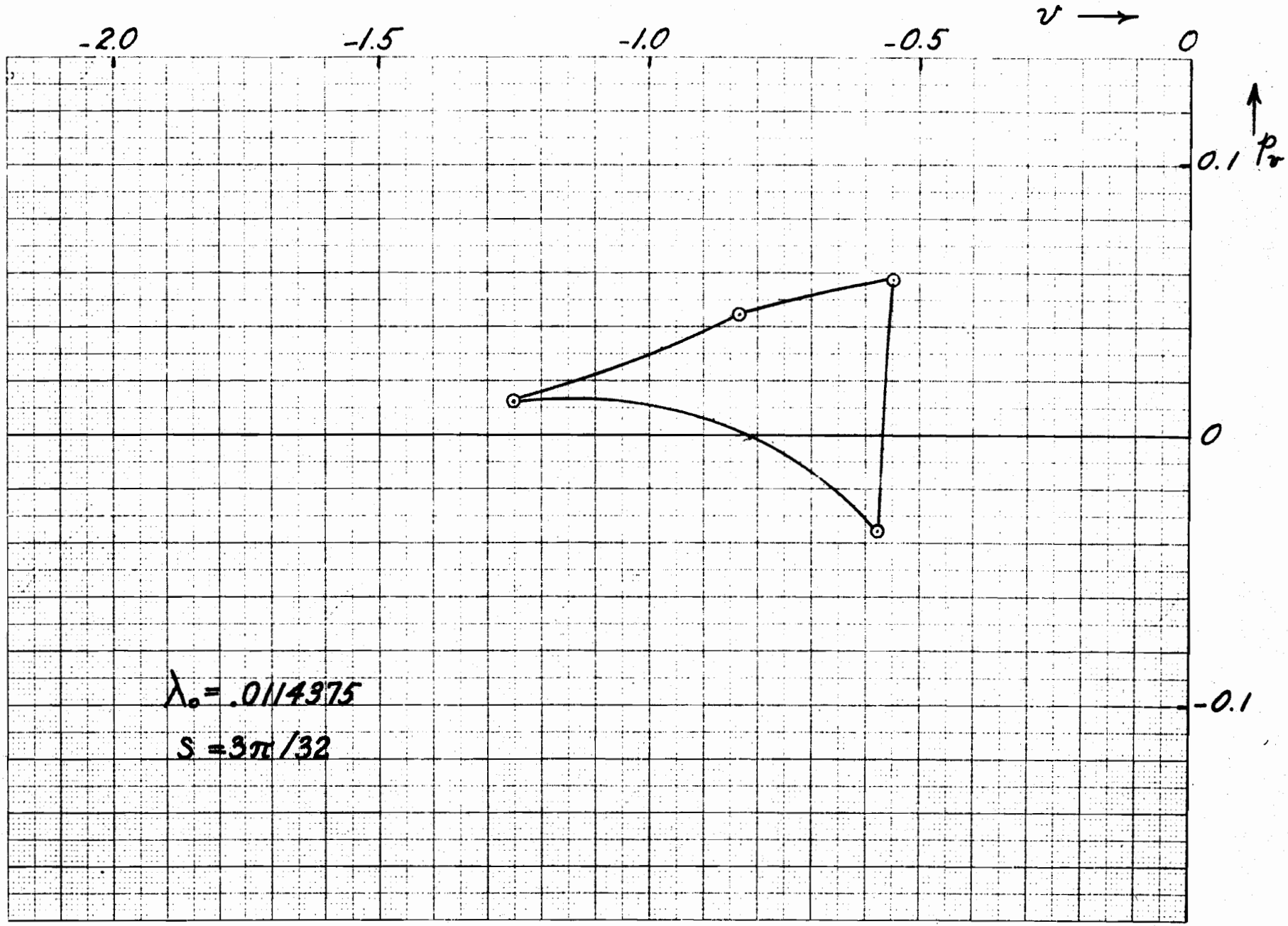

Fig. 24

EARPRINT PAPER CO. NO. C39. MILLIMETERS BOTH WAYS 160 X 220 DIVISIONS CLEARPRINT CHARTS PRINTED IN U.S.A. ON CLEARPRINT TECHNICAL PAPER NO. 1000H

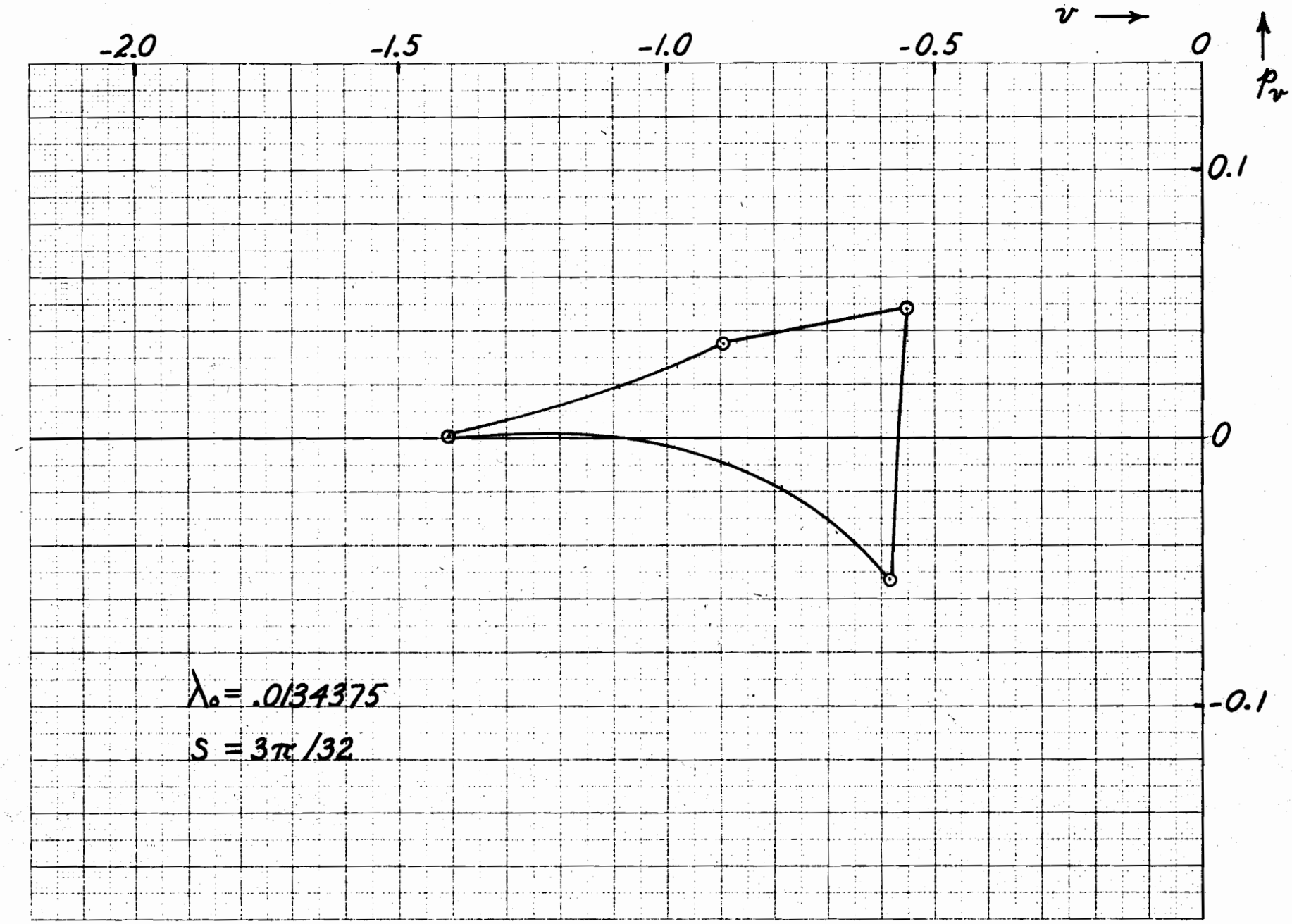

Fig. 25

CLEARPRINT PAPER CO. NO. C39. MILLIMETERS BOTH WAYS 160 X 220 DIVISIONS. CLEARPRINT CHARTS PRINTED IN U.S.A. ON CLEARPRINT TECHNICAL PAPER NO. 1000

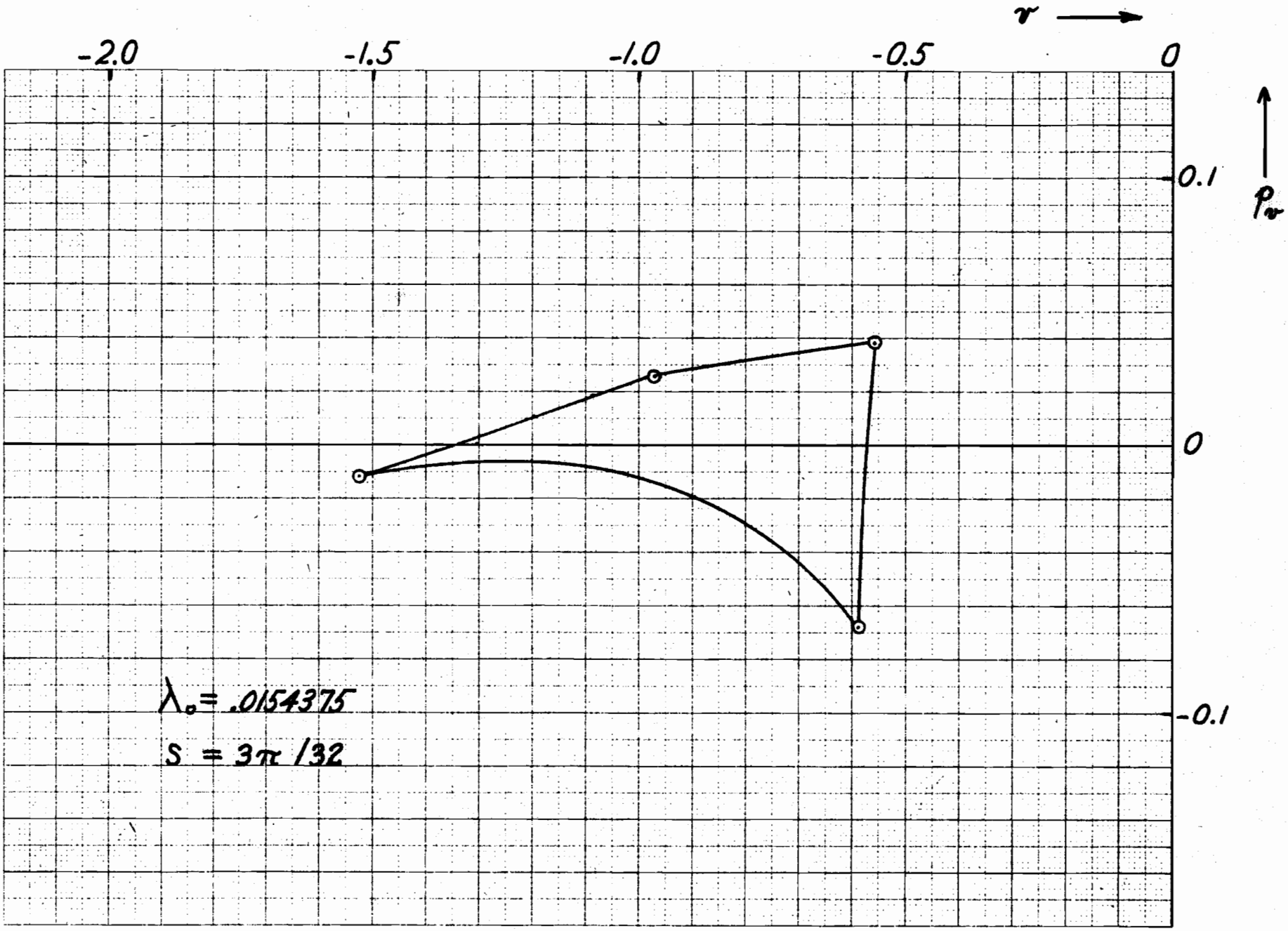

Fig. 26

CLEARPRINT PAPER CO. NO. C39 MILLIMETERS BOTH WAYS 160 X 220 DIVISIONS PRINTED IN U.S.A. ON CLEARPRINT TECHNICAL PAPER NO. 1000H
CLEARPRINT CHARTS

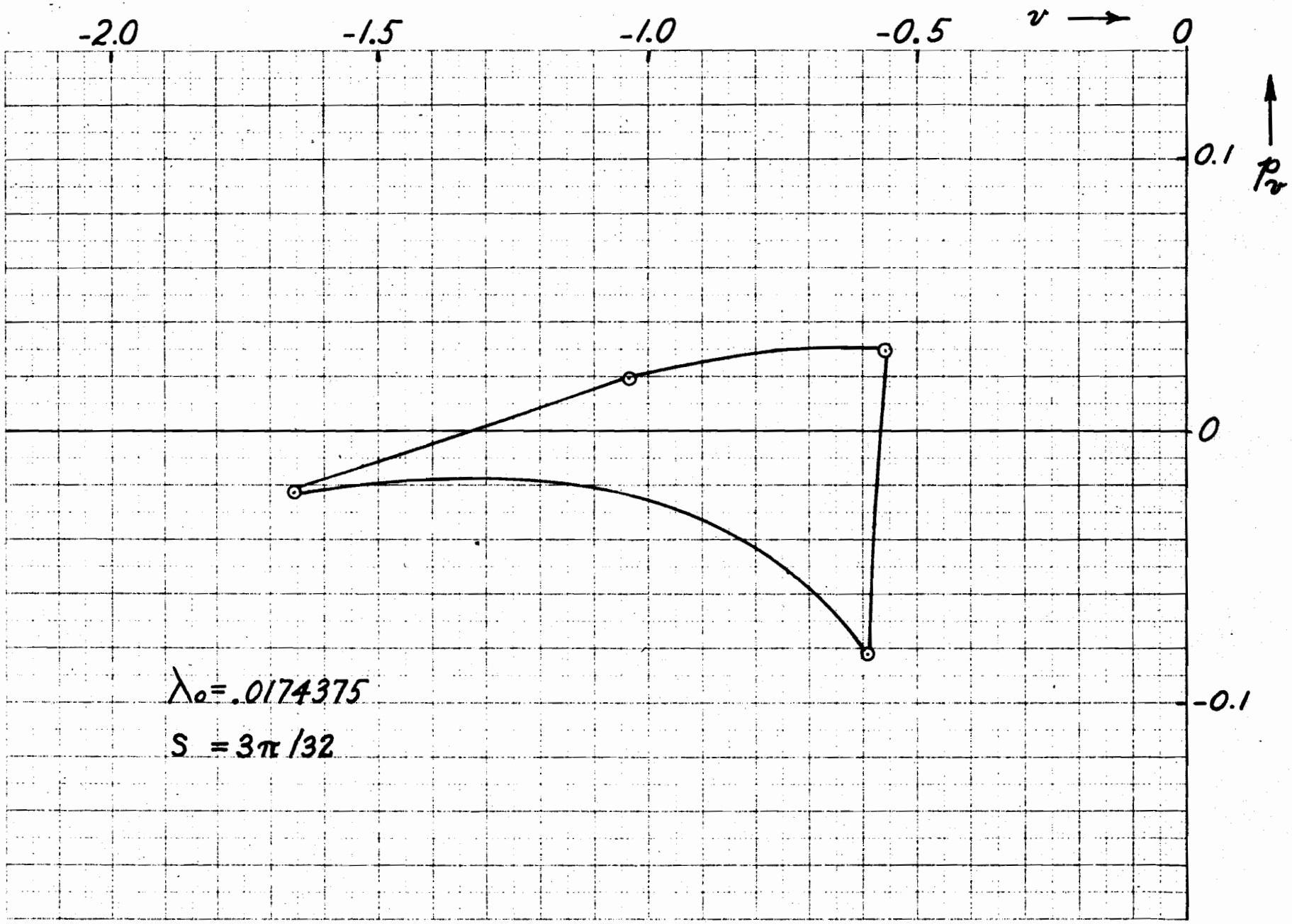

Fig. 27

ARPRINT PAPER CO NO. C39. MILLIMETERS BOTH V. 10 X 220 DIVISIONS. PRINTED IN U.S.A. ON CLEARPRINT TECHNICAL PAPER NO. 1000H CLEARPRINT CHARTS

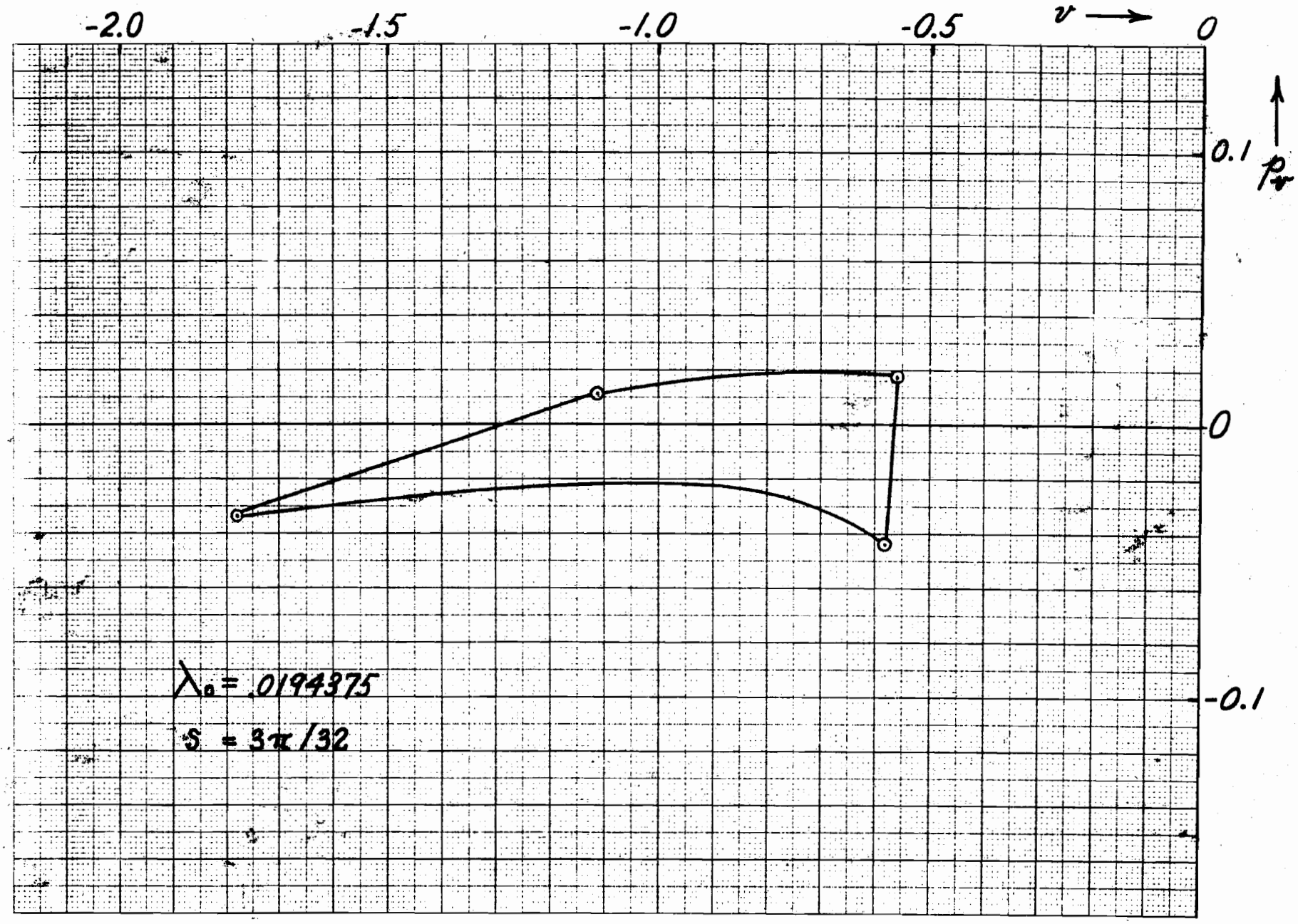

Fig. 28

CLEARPRINT PAPER CO. NO. C39. MILLIMETERS BOTH WAYS 160 X 220 DIVISIONS. PRINTED IN U.S.A. ON CLEARPRINT TECHNICAL PAPER NO. 1000H

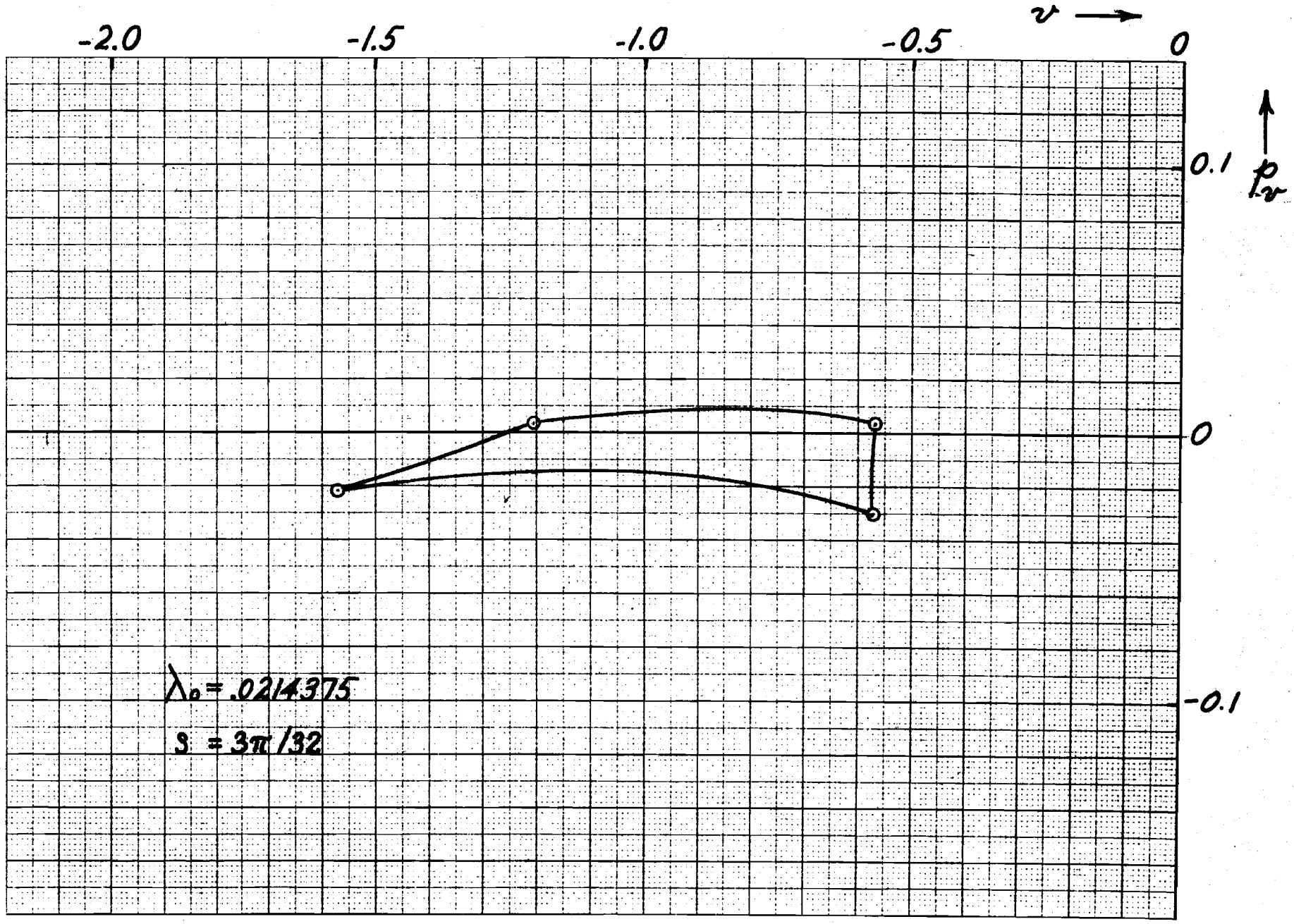

Fig. 29

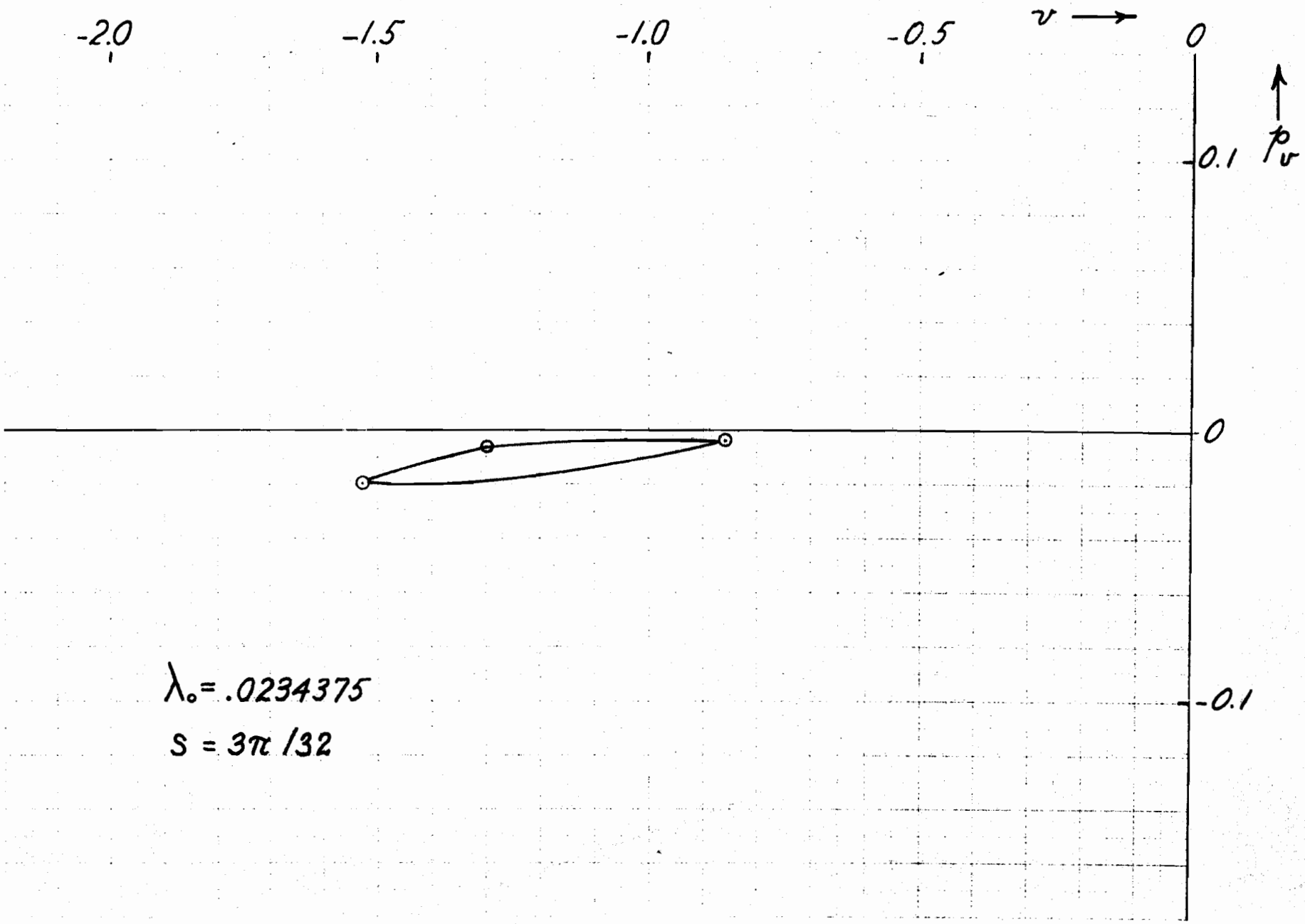

Fig. 30

CLEARPRINT PAPER CO. NO. C39 MILLIMETERS BOTH WAYS 160 X 220 DIVISIONS. PRINTED IN U.S.A. ON CLEARPRINT TECHNICAL PAPER NO. 1000H
CLEARPRINT CHARTS

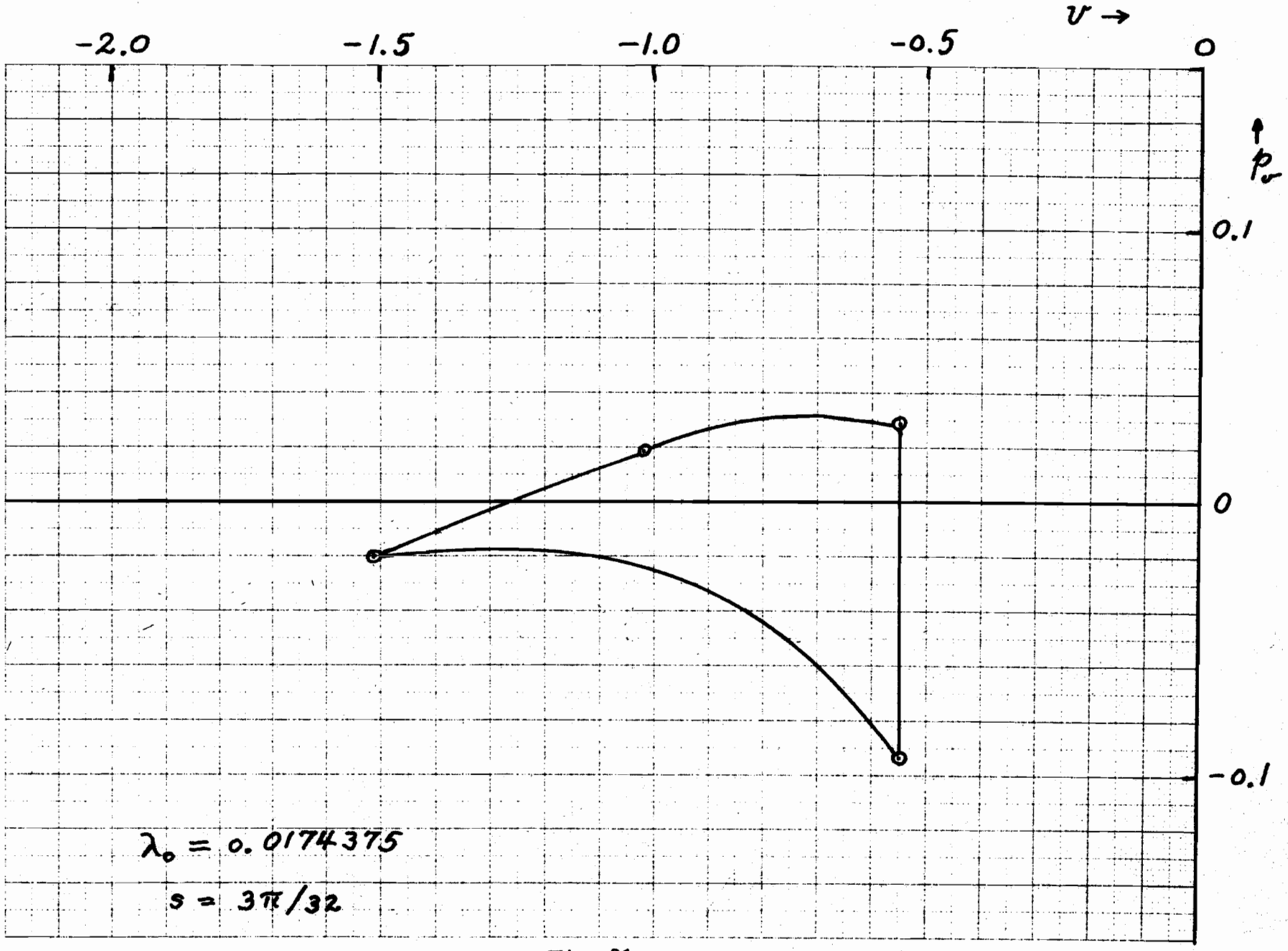

Fig. 31

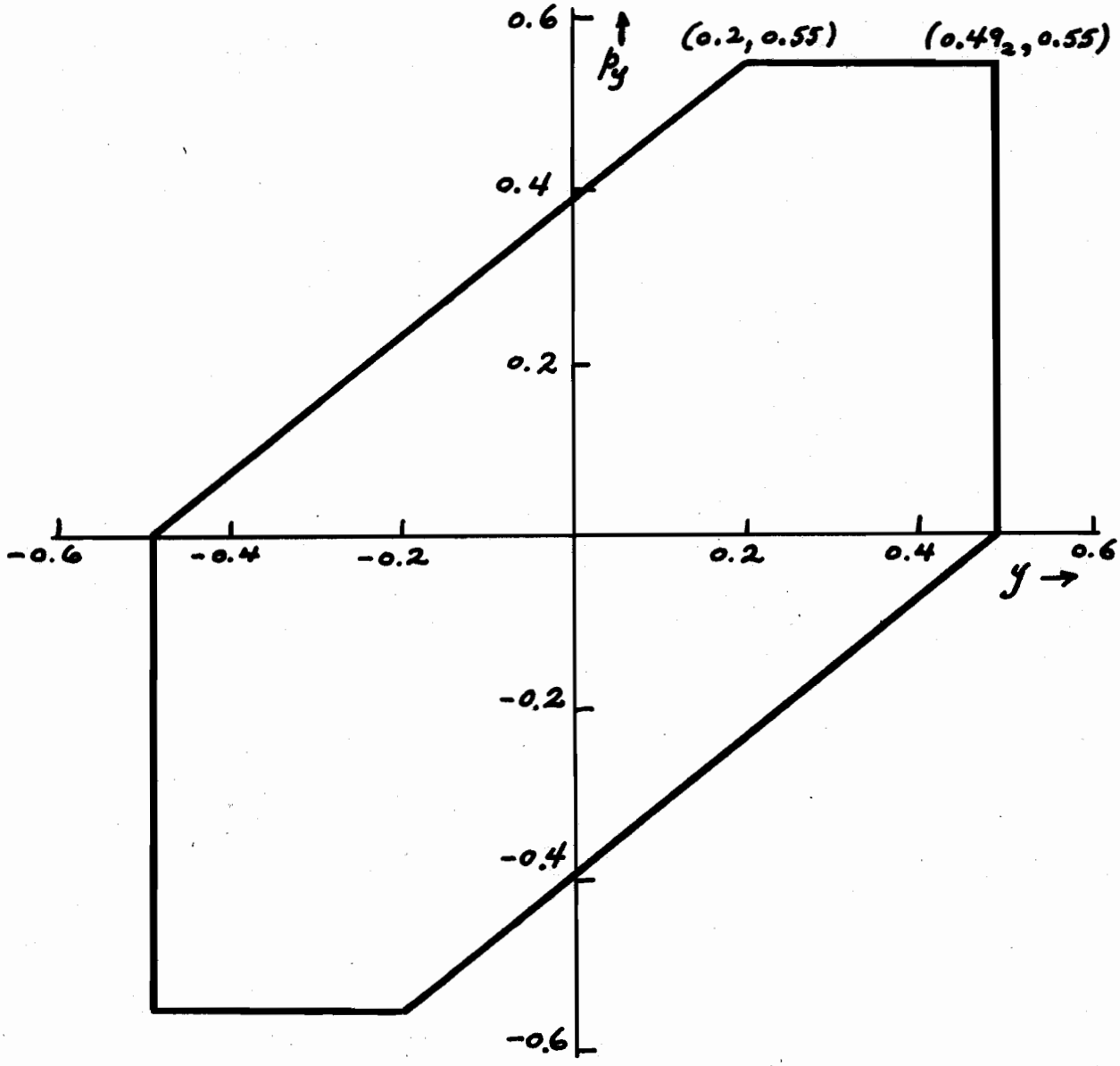

Fig. 32

CLEARPRINT PAPER CO. NO. C39X MILLIMETERS 200 BY 250 DIVISIONS
CLEARPRINT CHARTS

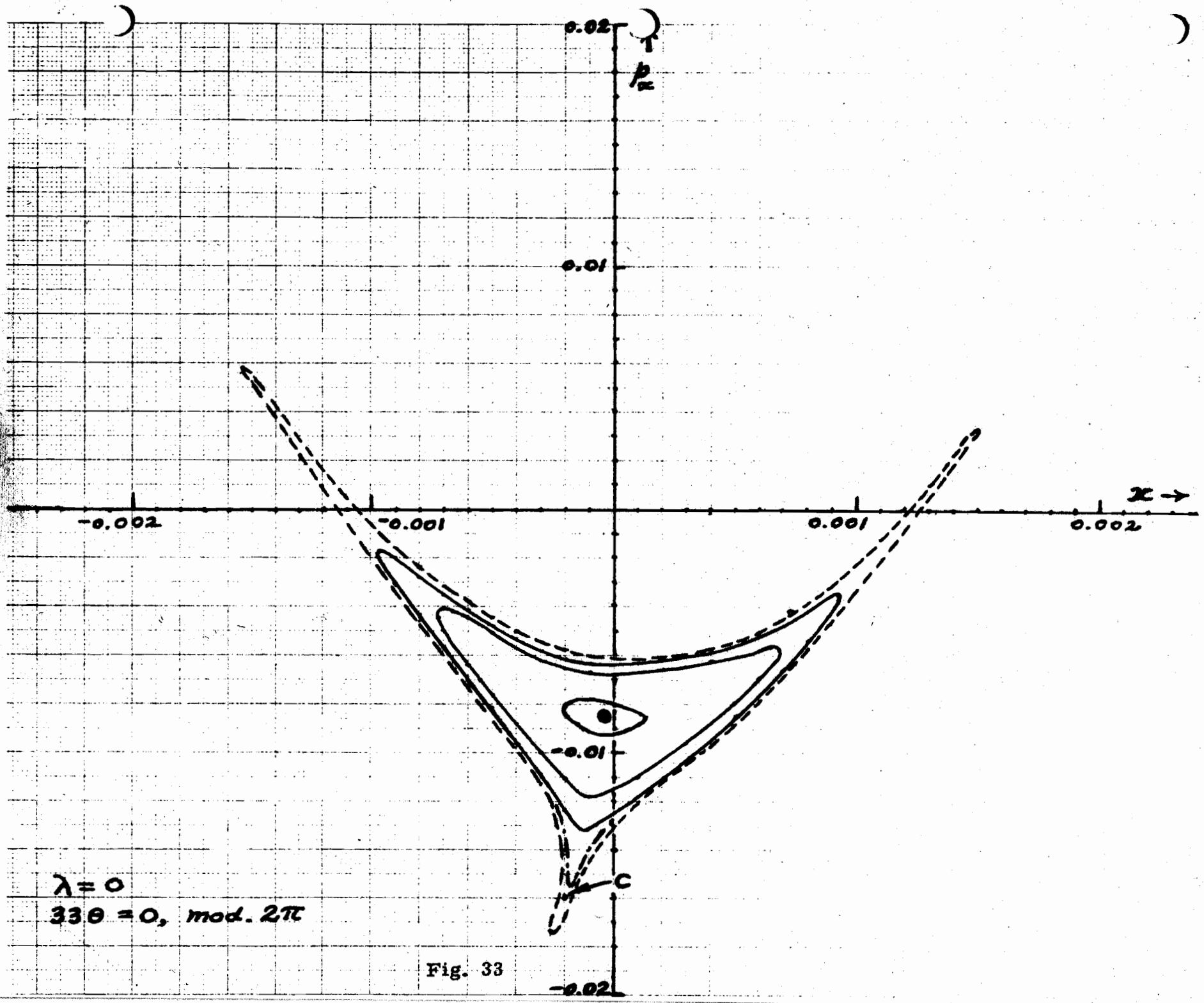

Fig. 33

CLEARPRINT CHARTS

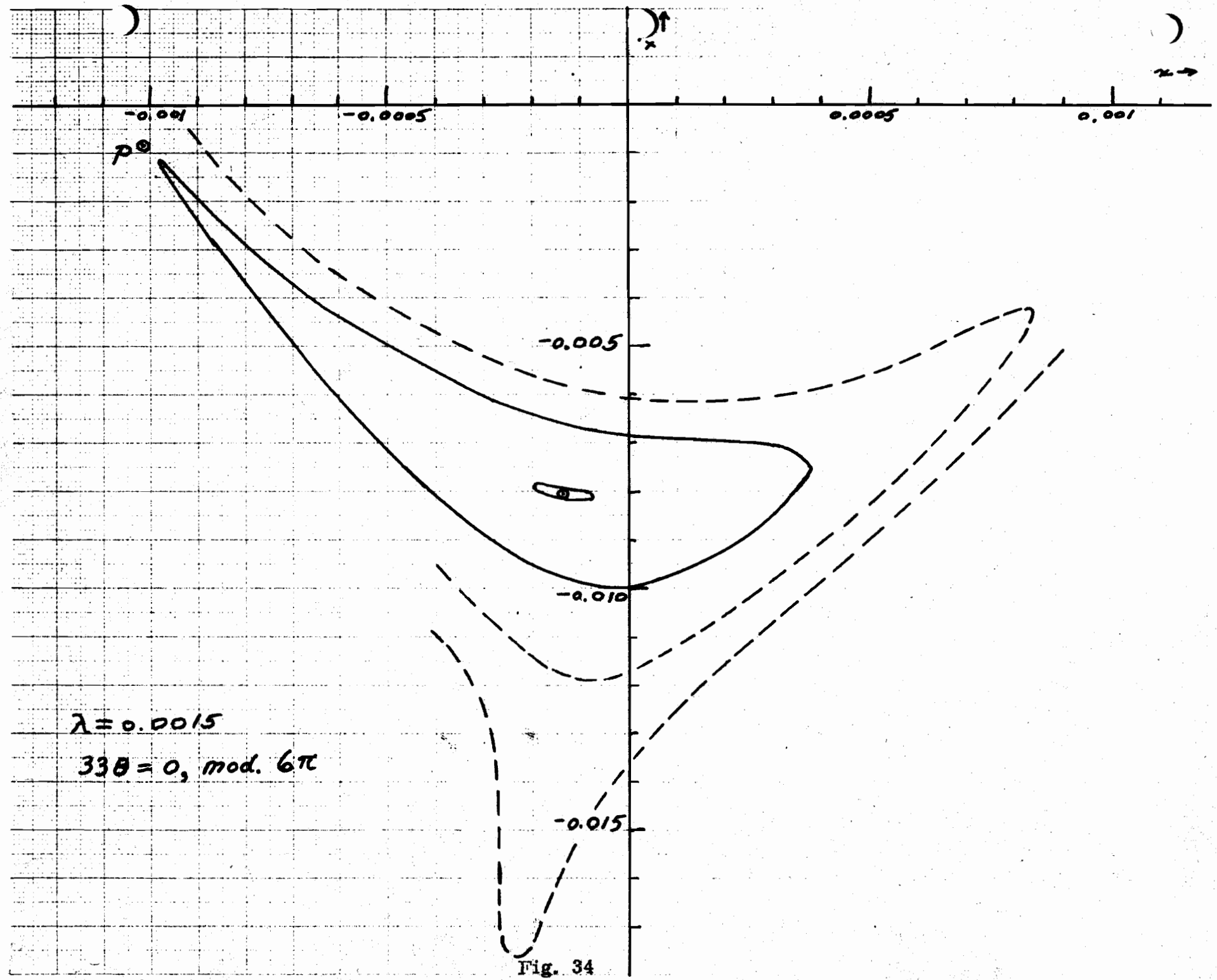

Fig. 34

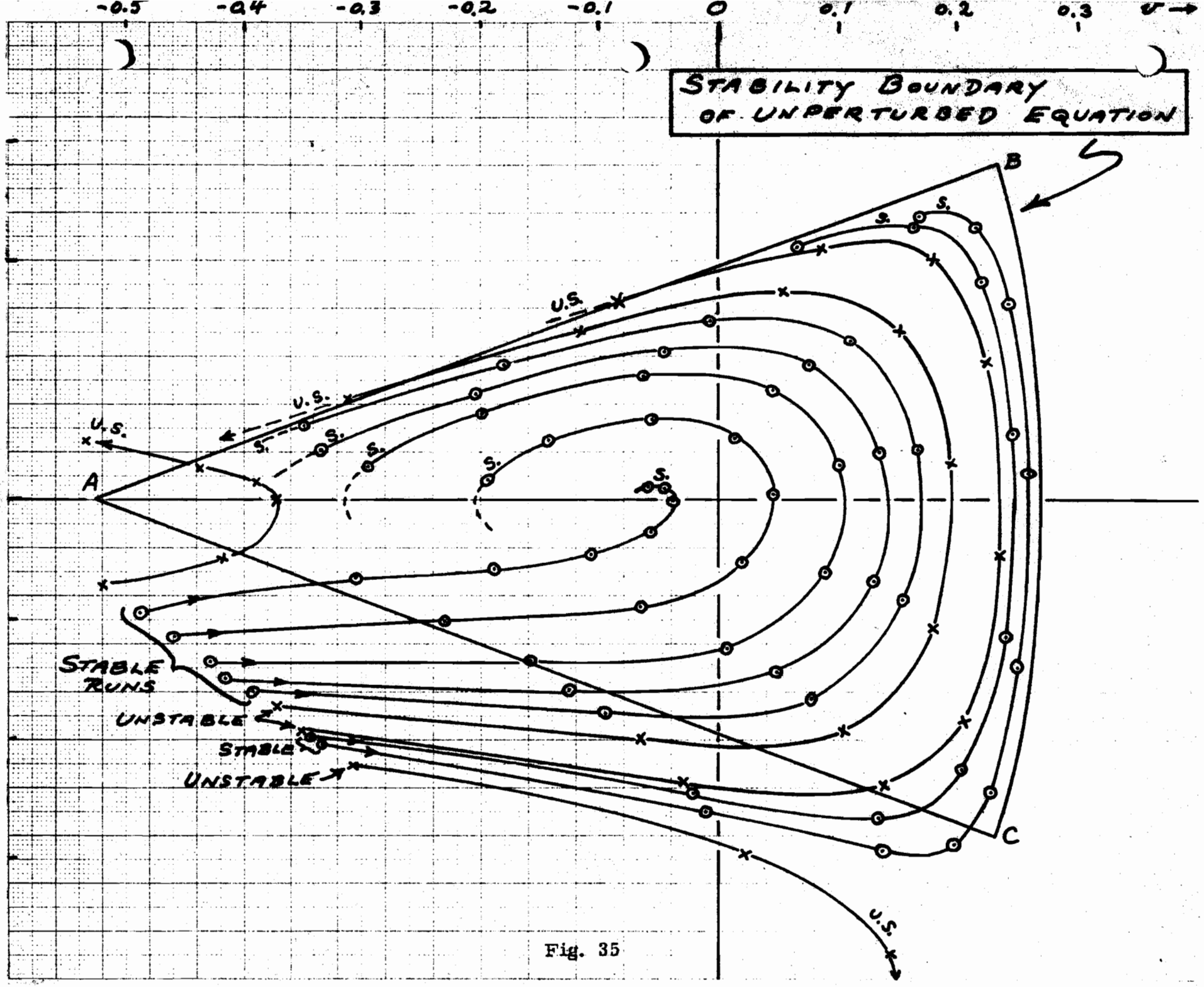
-0.5
-0.4
-0.3
-0.2
-0.1
0
0.1
0.2
0.3
v →
STABILITY BOUNDARY
OF UNPERTURBED EQUATION
A
B
C
U.S.
S.
STABLE
RUNS
UNSTABLE
STABLE
UNSTABLE

Fig. 35